



Global Sea Ice Concentration Climate Data Record Validation Report

OSI-450 and OSI-430-b

Version : 1.1

Date : 30/04/2019

Matilde Brandt Kreiner, John Lavelle, Rasmus Tonboe, Eva Howe
Danish Meteorological Institute

Thomas Lavergne, Mari Anne Killie, Atle Sørensen,
Steinar Eastwood, Amélie Neuville
Norwegian Meteorological Institute

Document Change record

Document version	Software version	Date	Author	Change description
1.0 - draft	5.2	17.02.2017	OSI SAF HL team	First draft version for DRR review
1.0	5.2	31.03.2017	OSI SAF HL team	First version for release after DRR review
1.1 - draft	5.2	23.01.2019	OSI SAF HL team	Updated with validation of OSI-430-b.
1.1	5.2	30.04.2019	OSI SAF HL team	Edited version after ORR review.

The software version number gives the corresponding version of the OSI SAF High Latitude software chain which was used to produce the reprocessing data set.

Table of contents

1. Introduction.....	5
1.1. <i>Scope of the document.....</i>	5
1.2. <i>Reference documents.....</i>	5
1.3. <i>Definitions, acronyms and abbreviations.....</i>	6
2. Sea ice products comparison.....	7
2.1. <i>OSI SAF Global Sea Ice Concentration data availability.....</i>	7
2.2. <i>Ice chart data availability.....</i>	7
2.3. <i>About ice chart data.....</i>	8
2.4. <i>Representation of ice chart information.....</i>	9
2.5. <i>Validation parameters.....</i>	10
2.6. <i>Requirements.....</i>	10
2.7. <i>Comparison between the OSI-450 product and NIC ice charts.....</i>	12
2.7.1. <i>Northern Hemisphere.....</i>	13
2.7.2. <i>Southern Hemisphere.....</i>	20
2.8. <i>Differences in validation for OSI-450 compared to OSI-409.....</i>	26
2.8.1. <i>Northern Hemisphere.....</i>	27
2.8.2. <i>Southern Hemisphere.....</i>	31
2.9. <i>Comparison between the OSI-430-b and NIC ice charts.....</i>	35
2.9.1. <i>Northern Hemisphere.....</i>	35
2.9.2. <i>Southern Hemisphere.....</i>	38
2.10. <i>Differences in validation for OSI-430-b compared to OSI-450 and OSI-430.....</i>	41
2.10.1. <i>Northern Hemisphere.....</i>	41
2.10.2. <i>Southern Hemisphere.....</i>	44
3. Comparison of sea ice area and extent monthly trends.....	47
3.1. <i>SIC CDR data sources.....</i>	47
3.1.1. <i>OSISAF CDR v2 : OSI-450 and OSI-430-b.....</i>	47
3.1.2. <i>OSISAF CDR v1 : OSI-409 and OSI-430 series.....</i>	47
3.1.3. <i>NSIDC SIC CDR V2 :.....</i>	47
3.2. <i>Definitions and Methodology.....</i>	47
3.2.1. <i>Indicators and trends.....</i>	47
3.2.2. <i>Gap-filling and interpolation of missing daily SIC values.....</i>	48
3.2.3. <i>Grids, Projections, land-masks, and climatologies.....</i>	48
3.3. <i>Results.....</i>	49
3.3.1. <i>Northern Hemisphere SIE.....</i>	49

3.3.2. Northern Hemisphere SIA.....	50
3.3.3. Southern Hemisphere SIE.....	51
3.3.4. Southern Hemisphere SIA.....	52
3.4. Continuity of SIE and SIA time-series with OSI-430-b.....	53
3.5. Discussion.....	54
4. Monitoring stability and internal consistency.....	55
4.1. Long-term stability.....	55
4.2. Transition from OSI-450 to OSI-430-b, and stability of OSI-430-b.....	56
5. Conclusions.....	58
6. Appendix.....	61

1. Introduction

1.1. Scope of the document

OSI-450 is the second major version of the OSI SAF Global Sea Ice Concentration Climate Data Record (CDR). The first version, OSI-409, was initiated in 2006 through visiting scientist activities with the UK Met Office and NSIDC, and was released in 2011. It was extended with OSI-409-a in 2015, using operational SSMIS and ECMWF data after 2009, but keeping the algorithms and processing chains unchanged. In this report OSI-409 + OSI-409-a is treated as one data record, labelled OSI-409.

OSI-450 is a full reprocessing of sea ice concentration, with improved algorithms and an upgraded processing chain, covering the period 1979 to 2015. The validation results of the OSI SAF global reprocessed sea ice concentration product OSI-450 version 1.0 is presented in this validation report and compared to those of the OSI-409, to show its relative improvements.

The OSI-430 is the sea ice concentration continuous reprocessing product ICDR v.1, that has operationally extended the OSI-409 (and OSI-409-a) from 2015-. The OSI-430-b is the sea ice concentration ICDR v.2 with an improved algorithm, that operationally extends the OSI-450 and will be the new continuously updated OSI SAF sea ice concentration CDR. The validation results of the OSI-430-b is presented in this report to show the temporal consistency to the OSI-450 CDR. Moreover, the OSI-430-b validation results are compared to those of the predecessor, OSI-430, to show its relative improvements.

The validation report describes a comparison between OSI SAF ice concentrations derived from satellite microwave radiometer data and ice charts produced manually on the basis of satellite and reconnaissance data for ship navigation support. The OSI SAF product is compared to National Ice Center (NIC) ice charts for both hemispheres. The validation report also presents sea ice extent and area monthly trends derived from the OSI SAF products.

All intellectual property rights of the OSI SAF products belong to EUMETSAT. The use of these products is granted to every interested user, free of charge. If you wish to use these products, EUMETSAT's copyright credit must be shown by displaying the words "Copyright © 2018 EUMETSAT" on each of the products used.

1.2. Reference documents

- [1] OSI SAF
Product Requirements Document
SAF/OSI/CDOP2/M-F/MGT/PL/2-001, version 3.7, 07/11/2016
- [2] OSI SAF
Global Sea Ice Concentration Climate Data Record Product User Manual, OSI-450
SAF/OSI/CDOP2/MET/TEC/MA/288, version 1.0, 22/03/2017
- [3] OSI SAF
Validation Report for *Global Sea Ice Concentration Reprocessing Product OSI-409, OSI-409a and OSI-430*
SAF/OSI/CDOP2/DMI/SCI/RP/226, version 2.0, 29/04/2015

- [4] OSI SAF
Global Sea Ice Concentration Climate Data Record Justifications of Requirements, OSI-450 SAF/OSI/CDOP2/DMI/TEC/TN/241, version 1.1., 16/11/2015
- [5] Meier, W., F. Fetterer, M. Savoie, S. Mallory, R. Duerr, and J. Stroeve.
NOAA/NSIDC Climate Data Record of Passive Microwave Sea Ice Concentration, Version 2. [goddard_merged_seaice_conc]. Boulder, Colorado USA. National Snow and Ice Data Center. doi: <http://dx.doi.org/10.7265/N55M63M1>. 2013, updated 2016. , Rathmann, N., Dybkjær, G., Pedersen, L. T., Høyer, J. L., and Kern, S.:

The EUMETSAT sea ice concentration climate data record
The Cryosphere, 10, 2275-2290, doi:10.5194/tc-10-2275-2016, 2016.
- [7] Fennig, K., Schröder, M., and Hollmann, R.: Fundamental Climate Data Record of Microwave Imager Radiances, Edition 3, Satellite Application Facility on Climate Monitoring, doi:10.5676/EUM_SAF_CM/FCDR_MWI/V003, 2017.
- [8] Lavergne, T., Sørensen, A. M., Kern, S., Tonboe, R. T., Notz, D., Aaboe, S., Bell, L., Dybkjær, G., Eastwood, S., Gabarro, C., Heygster, G., Killie, A.M., Kreiner, M.B., Lavelle, J., Saldo, R., Sandven, S., Pedersen, L. T.:
Version 2 of the EUMETSAT OSI SAF and ESA CCI sea ice concentration climate data records
The Cryosphere, 13, 49-78, <https://doi.org/10.5194/tc-13-49-2019>, 2019.

1.3. Definitions, acronyms and abbreviations

AVHRR	Advanced Very High Resolution Radiometer
CDR	Climate Data Record
DMSP	Defence Meteorological Satellite Program
EASE	Equal-Area Scalable EarthSouthern Hemisphere
ECMWF	European Centre for Medium range Weather Forecast
FTP	File Transfer Protocol
ICDR	Interim Climate Data Record
MODIS	MODERate resolution Imaging Spectroradiometer
NH	Northern Hemisphere
NIC	National Ice Center
NWP	Numerical Weather Prediction
OLS	Optical Line Scanner (on DMSP)
OSI SAF	Ocean and Sea Ice SAF
SAF	Satellite Application Facility
SAR	Synthetic Aperture Radar
SH	Southern Hemisphere
SIGRID	Sea ice chart grid format
SIA	Sea ice area
SIE	Sea ice extent
SMMR	Scanning Multichannel Microwave Radiometer (on NIMBUS 7)
SSM/I	Special Sensor Microwave Imager
SSMIS	Special Sensor Microwave Imager Sounder

2. Sea ice products comparison

2.1. OSI SAF Global Sea Ice Concentration data availability

The OSI SAF sea ice concentration products are distributed freely through the OSI SAF Sea Ice FTP server. The data are organized in year and month directories.

The OSI-450 Climate Data Record product is available for the period 1979 (OSI-450 will go back to 1979 only, justified by the late start of ERA-Interim data) to 2015 at this address:

<ftp://osisaf.met.no/reprocessed/ice/conc/v2p0>

The OSI-430-b Interim Climate Data Record product is available for the period 2015 and onwards at this address:

<ftp://osisaf.met.no/reprocessed/ice/conc-cont-reproc/>

The spatial sampling of the sensors used in the OSI SAF products is not sufficient for the daily sea ice concentration fields to be presented at 10 or 12.5km resolution without dedicated additional work on the processing algorithms and/or uncertainties. An EASE2 grid with 25 km resolution is a more sensible spatial sampling for these products.

Some of the daily sea ice concentration products have not been produced as a result of missing satellite data (due to satellite malfunction, planned maintenance or missing archive). The SMMR instrument was operated every second day. More details on this is provided in the Product User Manual [RD-1]. Below are listed the different satellite missions and the periods they are used for OSI-450 and OSI-430-b.

Sensor	Data since	End
Nimbus 7 SMMR	October 1978	August 1987
DMSP F8 SSMI	July 1987	December 1991
DMSP F10 SSMI	January 1991	November 1997
DMSP F11 SSMI	January 1992	December 1999
DMSP F13 SSMI	May 1995	December 2008
DMSP F14 SSMI	May 1997	August 2008
DMSP F15 SSMI	December 1999	July 2006
DMSP F16 SSMIS	November 2005	2018
DMSP F17 SSMIS	December 2006	2018
DMSP F18 SSMIS	March 2010	2018

2.2. Ice chart data availability

This validation report describes a comparison between the OSI SAF ice concentrations derived from satellite microwave radiometer data and ice charts produced manually on the basis of satellite and reconnaissance data for ship navigation support.

A list of ice chart availability during the OSI SAF ice concentration reanalysis period follows. All ice charts are produced by the National Ice Center (<http://www.natice.noaa.gov/>). Ice chart data files have been acquired from different online data archives.

Hemi sphere	Period	Frequency	Format
North	1978 – 2014	Every second week 1978 – Jul. 1987 Weekly Jul. 1987 – Jun. 2001 Every second week Jun. 2001 – Oct. 2013 Twice a week Oct. 2013 – 2018	Binary files, 1972 – 2007, from ftp://sidads.colorado.edu . Shapefiles, 2006 - 2018 (2003-2006 in other format), from http://www.natice.noaa.gov .
South	1978 – 1994 and 2006 – 2014	Every second week 1978 – Jun. 1987 Weekly Jul. 1987 – Dec. 1994 Every second week Jan. 2006 – Oct. 2013 Weekly Oct. 2013 – 2018	SIGRID shapefiles, 1973 – 1994, from http://wdc.aari.ru . Shapefiles, 2006 - 2018 (2003-2006 in other format), from http://www.natice.noaa.gov .

2.3. About ice chart data

The OSI SAF global sea ice concentration reprocessed products are compared to the National Ice Center (NIC) ice charts, which are considered a relatively independent source of ice information.

Since 1972, NIC has produced ice charts on a regular basis covering all seasons, for both Southern and Northern Hemispheres. Thus, the time series cover the entire OSI SAF reanalysis period (see table above) except for the period 1995 to 2006 in the Southern Hemisphere where we have been unable to acquire digital ice charts.

Ice charts are produced manually on the basis of all available satellite imagery, in-situ reports (ships and aircraft reconnaissance) and meteorological/oceanographic guidance data. The NIC ice charts are a compilation of the ice conditions over a period (see ice chart frequency in the table above), using any data up to 72 hours old. This applies both for the biweekly, weekly and twice-weekly ice charts. Therefore, the ice charts are composite charts rather than snapshots of the ice coverage on a certain day or time. The ice charts are primarily used for strategic and tactical planning within the offshore and shipping community. A detailed manual interpretation and mapping procedure is carried out by skilled (experienced and trained) ice analysts and the estimates of ice concentration in the charts are based on the subjective judgement of the analyst. Ice charts are more accurate and detailed at the ice edge than passive microwave data because they are often made using higher resolution data. Also, analysts pay particular attention to regions near the ice edge because the characteristics and extent of ice in the marginal ice zone are important for operations taking place within or near that region. Conversely, analysts generally do not characterize the central Arctic with as much attention to detail, because most of the time there are no supported operations there. Studies of the differences between ice charts from different Ice Centres covering the same region shows relatively large (up to 30%) discrepancies in ice

concentrations standard deviation of the differences especially at intermediate concentrations (see [RD-6] for further information and references).

It is important to realize that the relative accuracy and level of analysis detail varies considerably through the SIGRID data set. Early ice charts are partly based on the passive microwave data from SMMR and SMMI used in the OSI SAF reanalysis, together with visual/infrared sensor data e.g. from AVHRR and OLS. The more recent ice charts are based on optical data when daylight and cloud-free conditions occur (e.g. MODIS) and partly on satellite SAR data for the Northern Hemisphere (e.g. Radarsat since 1995). Passive microwave radiometer data (e.g. SSMIS, AMSR-2) is only used if and where none of the before mentioned data sources are available. Until 1996, NIC produced all ice charts using imagery in a hardcopy format and traditional cartography techniques. Early analysis shortfalls resulted from: 1) poor resolution of early hardcopy (analog) satellite imagery, 2) the absence of verifiable in-situ data and 3) the degradation of image quality due to the high frequency of clouds.

The recent improvement in NIC analysis capabilities can be attributed to three factors: 1) a progressive increase in volume of incoming satellite data, 2) an improvement in the resolution of data used in each analysis and 3) the ability to process and enhance remotely sensed data in digital format.

2.4. Representation of ice chart information

The OSI SAF ice concentration is compared with the ice charts CT (Total ice Concentration) code variable of the SIGRID and Shapefiles. The SIGRID code is the WMO standard for describing ice information in ice charts. The CT SIGRID variable used for comparison is the total ice concentration given by the ice chart.

The ice chart methodology allows for CT to be either rounded ice concentrations, i.e. 50%, or ice concentration intervals, i.e. 40-60%. This information is available in the ice chart SIGRID and shapefiles. The binary ice chart files provide only rounded ice concentrations, thus the ice concentration intervals originally given in the ice chart have been simplified to average values of the ice concentration interval bounds. See the above table of ice chart file format availability.

The ice chart and the OSI SAF product from the same day are gridded onto a common projection and resolution. The OSI-450 has a EASE2-grid projection in 25.0 km resolution. For the validation the OSI-409/OSI-409a was re-gridded from the original 12.5 km EASE1-grid into the 25.0 km EASE2-grid projection to have the same grid spacing for all data sets. Both the OSI-450 and OSI-409 are computed from passive microwave radiometer data that have a resolution coarser than the 25.0 km grid spacing, thus the re-gridding of OSI-409 is not expected to cause loss of information content nor effect the validation result.

Following this a cell by cell comparison is carried out. For each ice chart concentration the deviation between ice chart concentration and OSI SAF ice concentration is calculated. When an OSI SAF ice concentration lies within an ice chart concentration interval, the deviation is zero. When an OSI SAF ice concentration lies outside an ice chart concentration interval, the deviation from OSI SAF ice concentration to the closest ice chart concentration interval value is calculated.

OSI SAF ice concentration product interpolated grid cells (i.e. pole-hole) and monthly climatological maximum ice extent masks (cf. [RD-2]) are not included in the comparison analysis.

2.5. Validation parameters

The ice concentration deviations are grouped into categories, i.e. $\pm 10\%$ and $\pm 20\%$, and the percentage of grid cells in each category is calculated. Furthermore the bias and standard deviation are calculated as described in the table below. The bias and standard deviation are reported for three categories; *ice* (close ice, $>99\%$ ice concentration), for *water* (0% ice concentration) and for *intermediate* ice ($0\% < \text{ice concentration} \leq 99\%$). Validation statistics for all three categories are shown in this report, but the product target requirements addresses the *ice* and *water* categories only.

The parameters shown in the validation plots are defined as follows. The ice chart analysis concentration will be referred as IAC and OSI SAF ice concentration as OSIC:

Parameter	Description
match_10_pct	The fraction of grid cells where IAC shows ice and OSIC is within $\pm 10\%$ of the IAC.
match_20_pct	The fraction of grid cells where IAC shows ice and OSIC is within $\pm 20\%$ of the IAC.
ice_bias	Average of OSIC – IAC for all grid cells where IAC shows close ice, IAC $> 99\%$.
water_bias	Average of OSIC – IAC for all grid cells where IAC shows open water, IAC = 0% .
Intermediate_bias	Average of OSIC – IAC for all grid cells where IAC shows intermediate ice concentrations, $0\% < \text{IAC} \leq 99\%$.
ice_stddev	Standard deviation of OSIC – IAC for all grid cells where IAC shows close ice, IAC $> 99\%$.
water_stddev	Standard deviation of OSIC – IAC for all grid cells where IAC shows open water, IAC = 0% .
Intermediate_stddev	Standard deviation of OSIC – IAC for all grid cells where IAC shows intermediate ice concentrations, $0\% < \text{IAC} \leq 99\%$.

2.6. Requirements

The OSI SAF product requirement document [RD-1] states about the reprocessed sea ice data that:

OSI-PRD-PRO-205: The OSI SAF shall reprocess the time series of SMMR, SSM/I and SSMIS data back to 1978 to expand the time series of global sea ice products.

OSI-PRD-PRO-206: The OSI SAF shall test new methods for ensuring a climate consistent data set.

OSI-PRD-PRO-207: The OSI SAF shall improve the coverage of the existing sea ice concentration, edge and type products by adding interpolation in the coastal zone and the area close to the pole where there is no satellite data coverage.

All of these three requirements have been met at the completion of the OSI SAF global reprocessed sea ice concentration data set.

Further, the specific product requirements listed in the OSI SAF product requirement document table OSI-PRD-PRO-200 are applicable for three categories: A threshold accuracy of 15%, a target accuracy of 8% and an optimal accuracy of 5%. The “threshold” is the minimum requirement to be met to ensure that data are useful. The “optimal” is an ideal requirement above which further improvements are not necessary. The “target” is an intermediate level between “threshold” and “optimum” which, if achieved, would result in a significant improvement for the targeted application. These numbers are standard deviation of mismatch of OSI-450 sea ice concentration to ice chart analysis concentration, averaged over one year. The mismatch between sea ice concentration from ice charts and from passive microwave radiometers is expected to be largest in summer. These statistics are evaluated at both “water” (0% IAC) and “ice” (>99% IAC) cases, separately.

The [RD-4] document gives the details for the product requirements for OSI-450 and explains the reasons for having the requirements on the 'ice' and 'water' categories, and not the 'intermediate ice' category.

2.7. Comparison between the OSI-450 product and NIC ice charts

Comparisons between National Ice Center (NIC) ice charts and the OSI SAF reanalysis for Northern and Southern Hemispheres are shown in the following two sections. Unfortunately ice chart data for the Southern Hemisphere is lacking for the period 1994 – 2006.

'Match' in Figure 1 and Figure 8, 'Bias' in Figure 2 and Figure 9 and 'Stddev' in Figure 3 and Figure 20 all show a seasonal cycle with highest agreement between the data sets in winter (December-March on Northern Hemisphere and June-September on Southern Hemisphere) and a lower agreement in summer, when bias and standard deviations are higher, due to the effect of summer melt on the radiometer sensor data.

Overall, the above mentioned figures show that there is an increased accordance between the two data sets during the reanalysis period, especially in the transition from SMMR to SSMI data in summer 1987. For both hemispheres this coincides with an increase in NIC ice chart frequency from biweekly to weekly production. This is also thought to have a positive effect on the accordance between data sets. The correspondence between data sets improves at the end of the reanalysis period from late 2013 and on, also likely being a consequence of an increased ice chart frequency (see table in Section 2.2 for ice chart data set availability). For the Northern Hemisphere it seems that there is a transition towards better correspondence between data sets around 1995-96. This could partly be due to the introduction of Radarsat data, and due to the change in NIC ice chart methodology to digital techniques, mentioned in Section 2.3. In mid-2001 the NIC ice chart frequency goes from weekly to biweekly production for the Northern Hemisphere resulting in less fluctuations in the comparison, but does not seem to affect the accordance between data sets. The introduction of ice charts in shape-file format from 2006 and onwards seems to degrade the accordance between the data sets for Northern Hemisphere. The Southern Hemisphere figures are unfortunately lacking important information in the period 1994-2006, but it is clear that both the seasonal pattern is clearer and the correspondence between data sets are better after the data gap. This can most likely also be explained by some of the above mentioned topics.

Comparison results are also shown as seasonal averaged (winter and summer) ice concentration scatter plots, in Figure 4 and Figure 5 for Northern Hemisphere and Figure 11 and Figure 12 for Southern Hemisphere. Plots show that by far the largest fraction of corresponding ice concentrations are found in the highest (>90% ice) and lowest (<10% ice) intervals. Plots also show that in general OSI-450 products have lower ice concentrations than the ice charts, where the ice charts show ice. Also, the OSI-450 products show some ice where ice charts have open water (0% IAC). This is due to the radiometer ice concentration being affected by atmospheric noise which increases the ice concentration above zero, and not all of this is removed by the open water filter. Large differences for the intermediate ice concentrations (0% < IAC <= 99%) is partly linked to the temporal differences of the two data sets (OSI SAF being a daily product and ice charts being a compilation of the ice conditions over a period) together with the higher mobility of open ice. A reason for the lack of any data points in the category for OSIC (90,100] and IAC (80,90] for the Northern Hemisphere could be, that the ice chart concentration interval of 70-90% is heavily used (appear much more often than e.g. 80-90%) and this interval would go into the IAC (70,80] category.

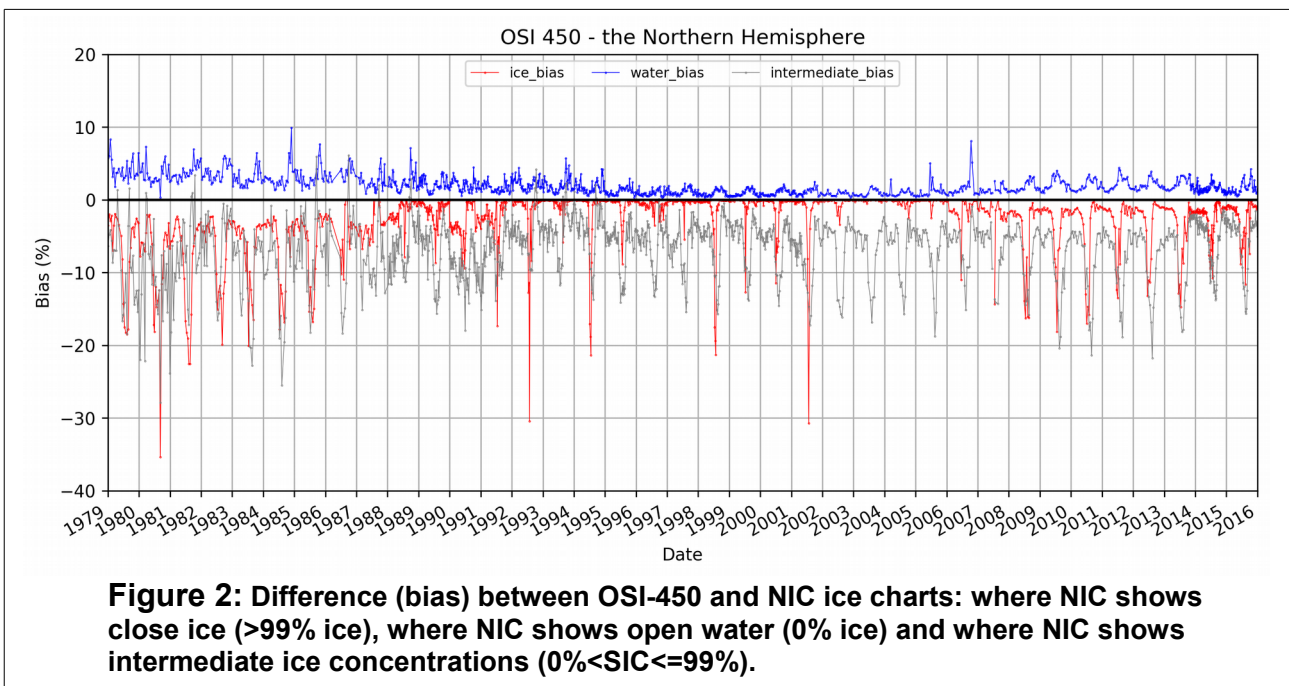
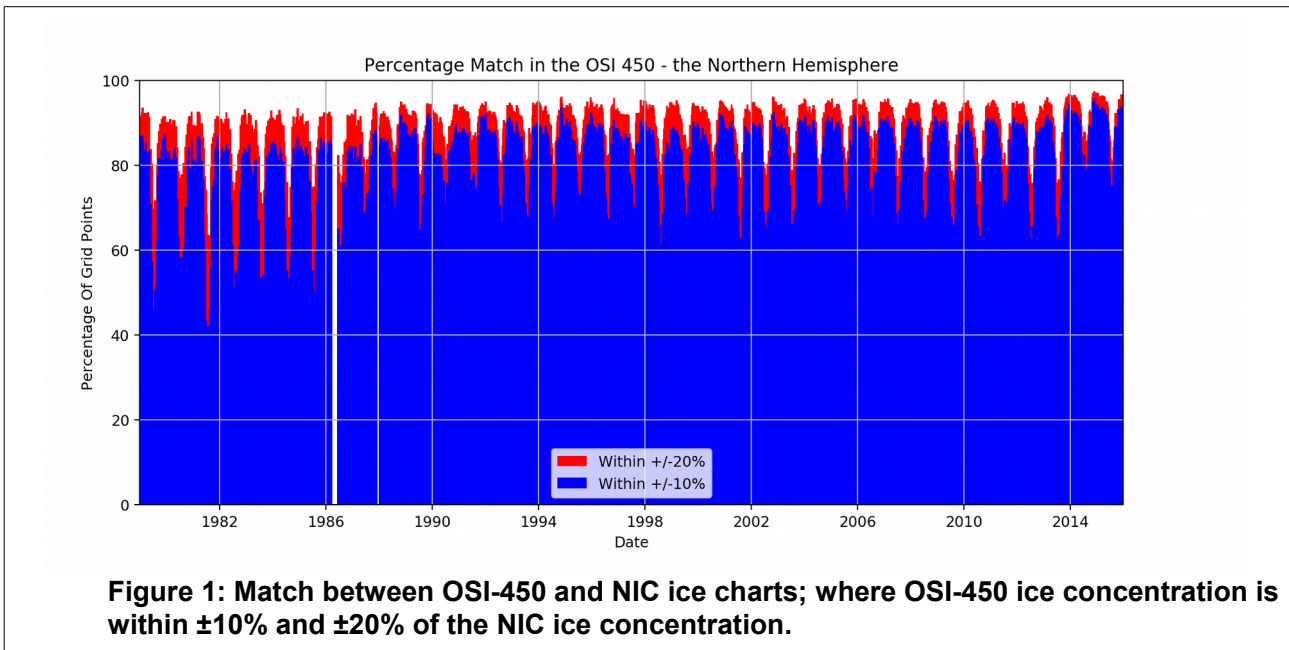
Maps of OSI-450 and ice chart seasonal median (winter and summer) OSICs and the corresponding IACs and their differences for the ice and water categories are shown in Figure 6 and Figure 7 for the Northern Hemisphere and Figure 13 and Figure 14 for the Southern Hemisphere. The bottom left plots

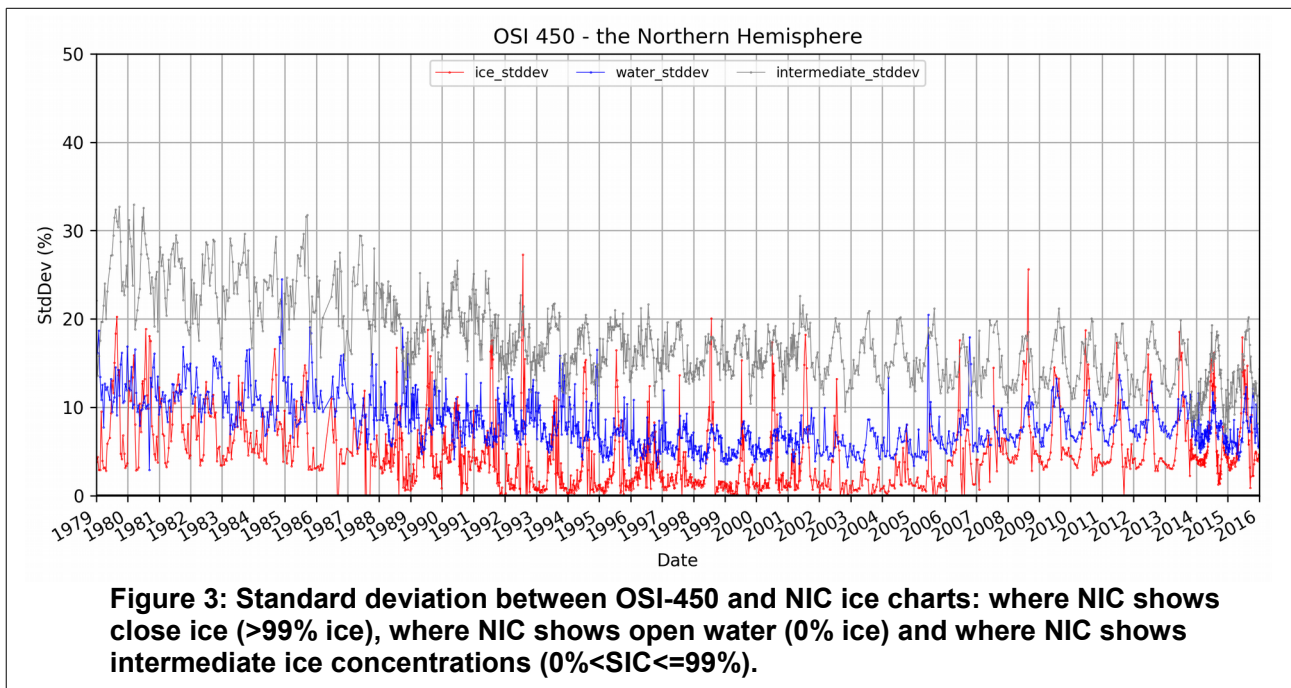
shows that differences in OSIC are predominantly found in a narrow (blue) band along the ice edge. (In a seasonal averaged plot the impact of spurious ice in the OSI-450 product caused by atmospheric water vapour is faded out). Also, bottom right plots show that the largest differences differences in OSI-450 (for IAC >99%) are in coastal areas, where land-fast ice occur (such as the Canadian Archipelago and along Northeast Greenland coast). These differences could also to some extent be explained by land spill-over effects. It is clear from Figure 6 that in winter OSI-450 has lower ice concentrations in the Arctic Ocean than given in the ice charts.

2.7.1. Northern Hemisphere

Figure 1 of percentage match shows a clear seasonal cycle with 80% to 95% of cases meeting the criteria during winter and 40% to 70% during the peak of summer melt. On average through the analysis period, 82% of the OSIC are within $\pm 10\%$ of the IAC and 90% lie within $\pm 20\%$. The difference (bias) in ice concentration in Figure 2 shows a positive water_bias at an average level of 2% through the reanalysis period. The interannual average bias for ice (>99% IAC) and intermediate ice (0% < IAC <=99%) is -2% and -7%, respectively. Both ice biases experience large fluctuations in summer. Figure 3 shows the standard deviation on the difference (bias) in ice concentrations, given in Figure 2. The yearly average standard deviation for the whole reanalysis period is 5% for close ice (>99% IAC), 17% for intermediate ice concentrations and 8% for open water (0% IAC). Yearly average and seasonal statistics (Dec.-Feb., Jun.-Aug., Mar.-May., Sep.-Nov.) are given in the table below:

OSI-450 NH	Match [%]		Bias [%]			Stddev [%]		
	within 10pct	within 20pct	ice	water	intermediate	ice	water	intermediate
Yearly average	82	90	-2	2	-7	5	8	17
DJF	88	94	-1	2	-5	3	8	15
JJA	70	82	-5	2	-11	9	8	20
MAM	86	92	-1	1	-5	4	7	17
SON	84	91	-2	2	-5	4	9	16





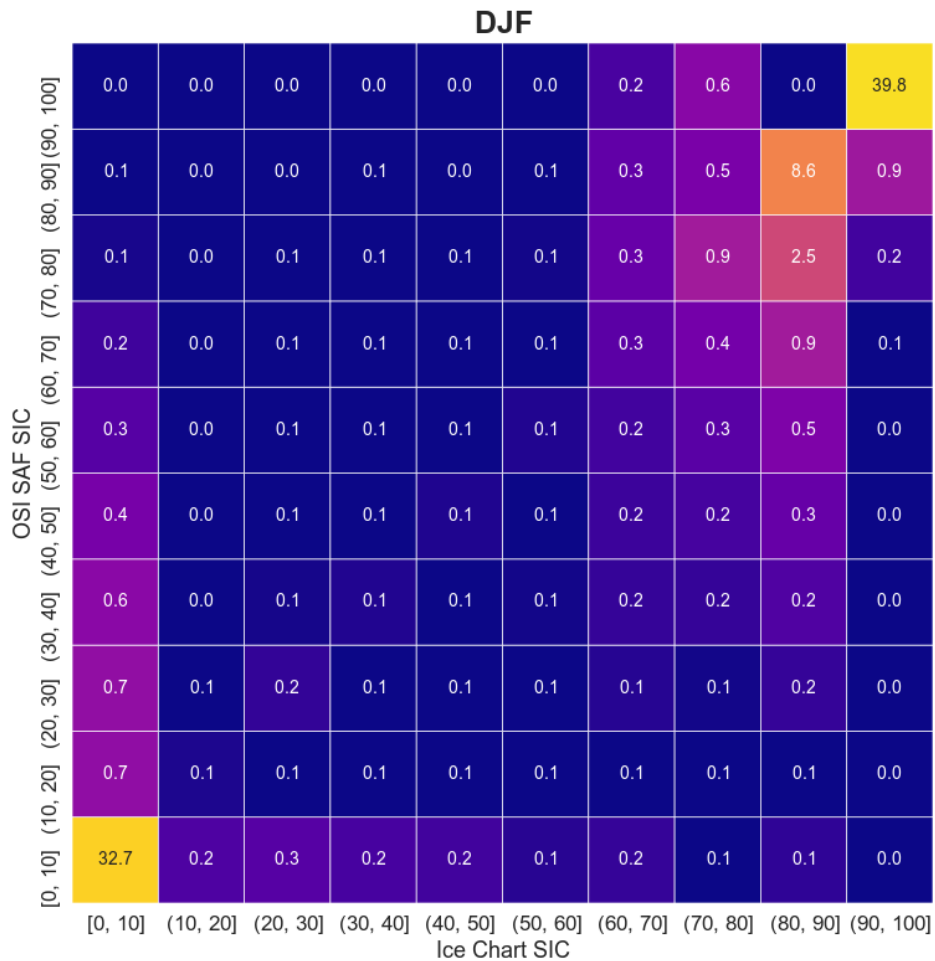


Figure 4: Density scatter plot of all corresponding OSI-450 and NIC ice chart ice concentrations in the grid point comparison, for Arctic winter in December, January and February [DJF]. White numbers are the percentage of grid points per ice concentration category [in logarithmic scale]. Ice concentration categories are defined by the open ('(') and closed ('[') boundaries.

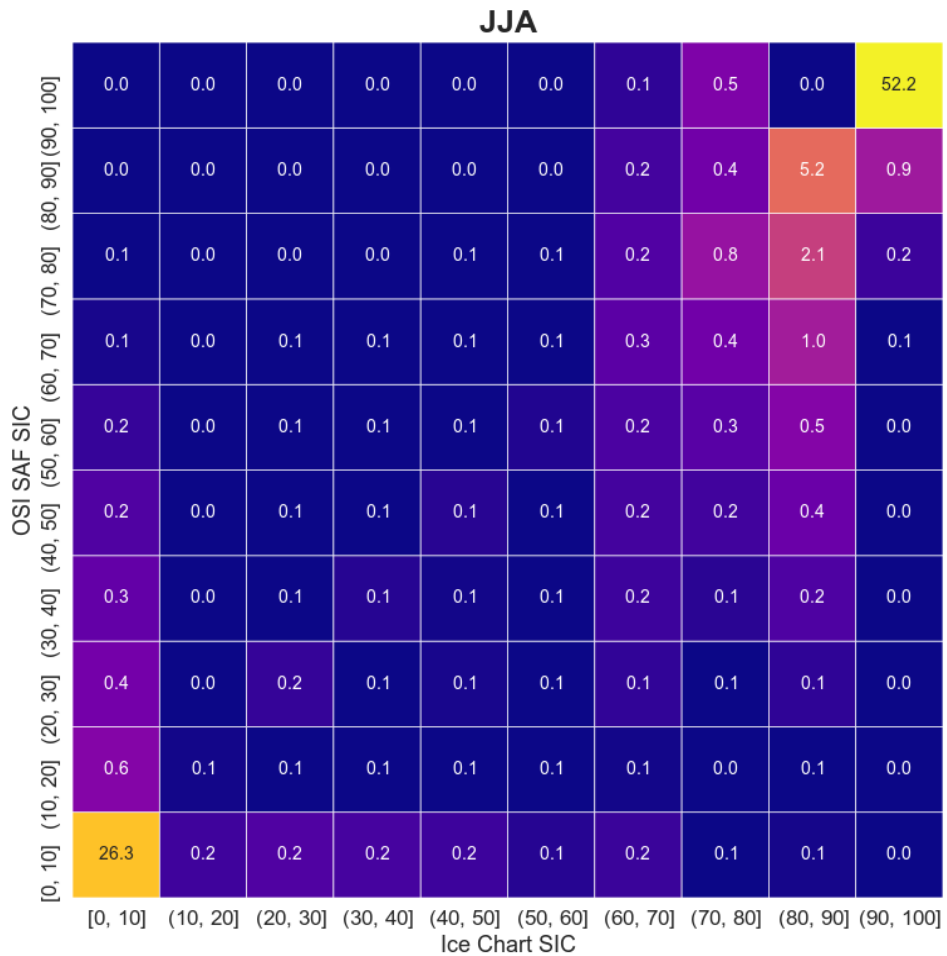


Figure 5: Density scatter plot of all corresponding OSI-450 and NIC ice chart ice concentrations in the grid point comparison. For Arctic summer in June, July and August [JJA]. White numbers are the percentage of grid points per ice concentration category [in logarithmic scale]. Ice concentration categories are defined by the open ('(') and closed ('[') boundaries.

Sea Ice Concentration (OSI SAF vs NIC) Comparison
DJF

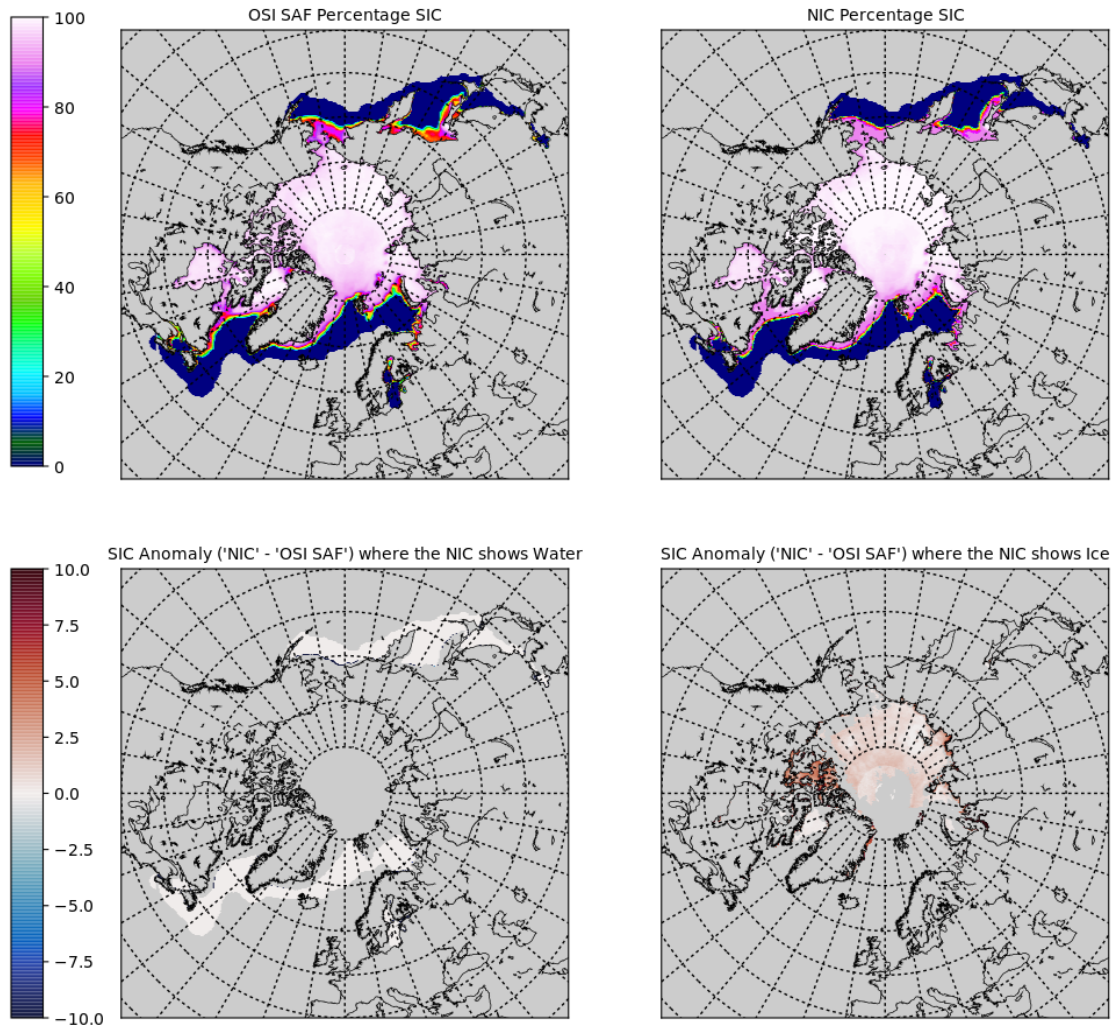


Figure 6: Map of Arctic winter season (December, January, February) median ice concentration of OSI-450 [top left] and of NIC ice charts [top right]. [bottom left] and [bottom right] show the ice concentration difference of OSI-450, where NIC ice concentrations are 0% ice and >99% ice, respectively.

Sea Ice Concentration (OSI SAF vs NIC) Comparison
JJA

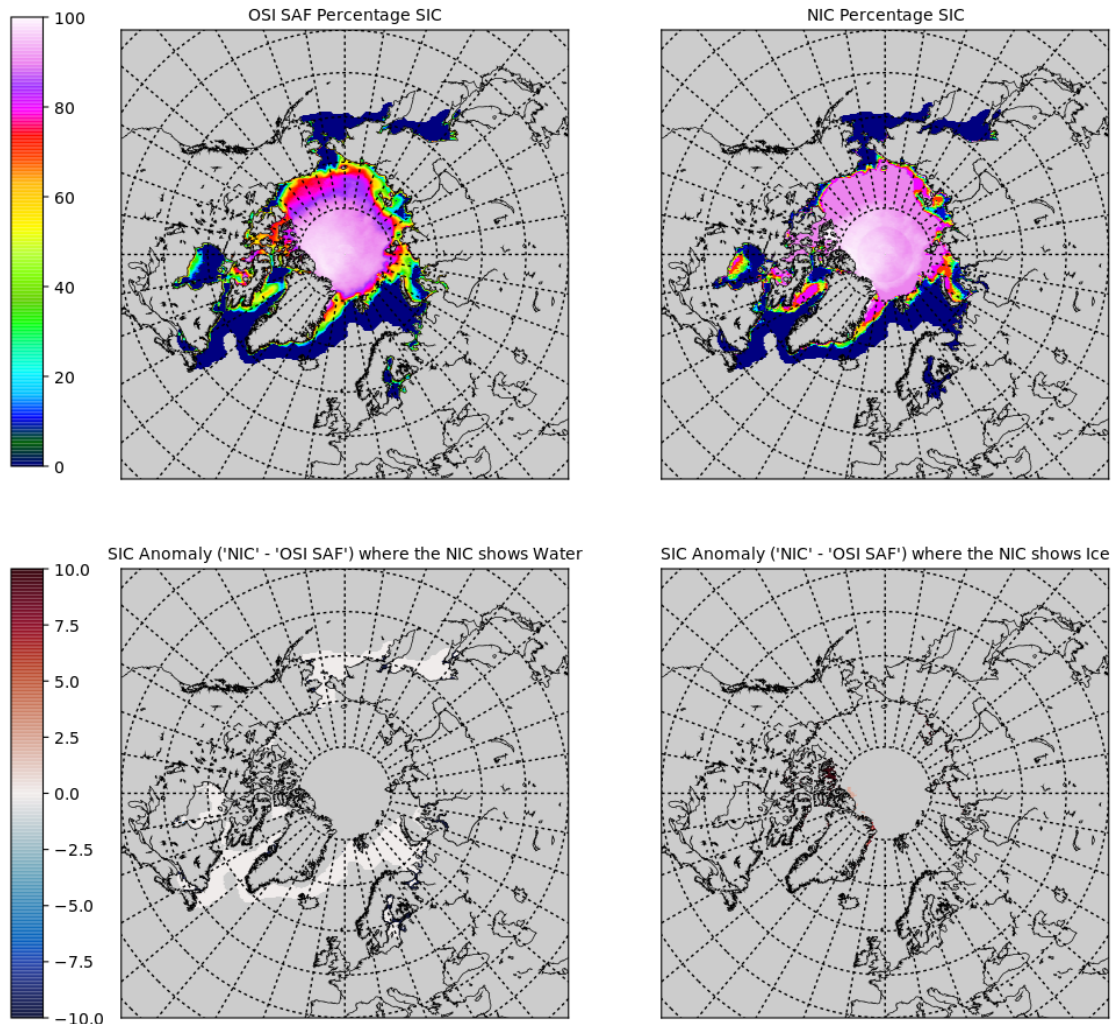


Figure 7: Map of Arctic summer season (June, July, August) median ice concentration of OSI-450 [top left] and of NIC ice charts [top right]. [bottom left] and [bottom right] show the ice concentration difference of OSI-450, where NIC ice concentrations are 0% ice and >99% ice, respectively.

2.7.2. Southern Hemisphere

Figure 8 shows the percentage match between data sets with a clear seasonal cycle of 80% to 95% of cases meeting the criteria during Antarctic winter and 70% to 80% during the peak of summer melt. On average through the analysis period, 85% of the OSI SAF grid point ice concentrations are within $\pm 10\%$ of the IAC and 90% lie within $\pm 20\%$. The difference (bias) in ice concentration in Figure 9 shows a positive water_bias at an average level of 1% through the reanalysis period. The water_bias is smaller than for the Northern Hemisphere which is most likely due to the difference in proportion of coastal zone to ocean waters; the Antarctic ice regime forms a broad band of ice around the continent, and there is not much coastal zone close to the ice edge/open water. This makes the ice edge more distinct and easier to detect by the radiometers and there is less land spill-over effect. The overall standard deviation of the difference in ice concentrations in Figure 10 decreases through the reanalysis period for all three categories. A minor exception is the small increase in Intermediate_stddev when switching from SMMR to SSMI in 1987. The comparison results are a bit more noisy in the first part of the period up till 1995 compared to the second part from 2006 and onwards. Yearly average and seasonal statistics (Dec.-Feb., Jun.-Aug., Mar.-May., Sep.-Nov.) are given in the table below:

OSI-450 SH	Match [%]		Bias [%]			Stddev [%]		
	within 10pct	within 20pct	ice	water	intermediate	ice	water	intermediate
Yearly average	85	90	-5	1	-10	10	7	18
DJF	82	88	-6	1	-13	13	6	21
JJA	87	92	-3	2	-7	8	8	16
MAM	85	90	-6	1	-11	12	6	19
SON	85	91	-4	1	-8	9	7	15

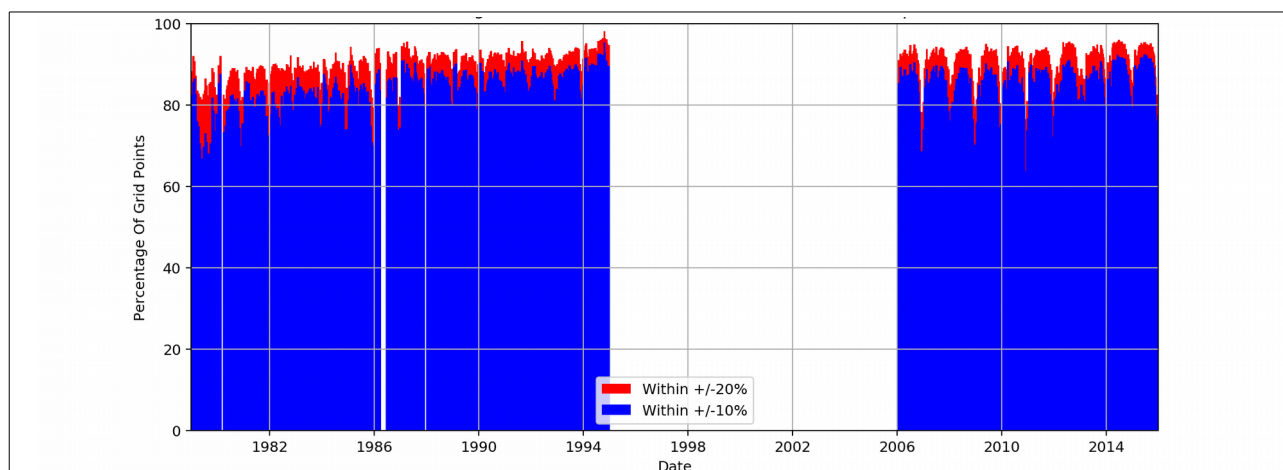


Figure 8: Southern Hemisphere match between OSI-450 and NIC ice charts; where OSI-450 ice concentration is within $\pm 10\%$ and $\pm 20\%$ of the NIC ice concentration.

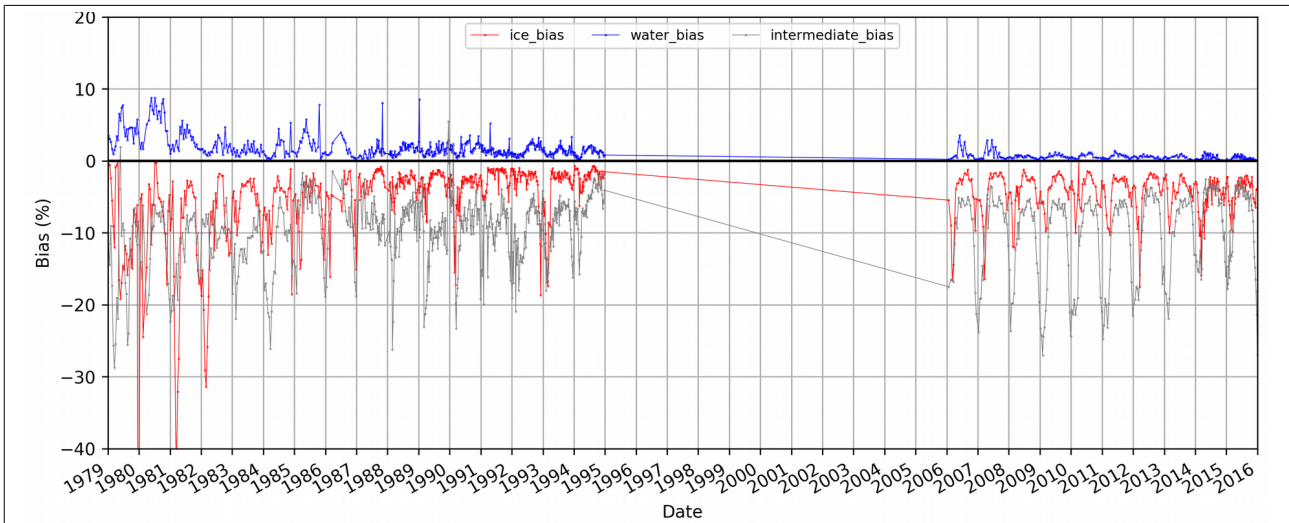


Figure 9: Southern Hemisphere difference (bias) between OSI-450 and NIC ice charts: where NIC shows close ice (>99% ice), where NIC shows open water (0% ice) and where NIC shows intermediate ice concentrations (0%<SIC<=99%).

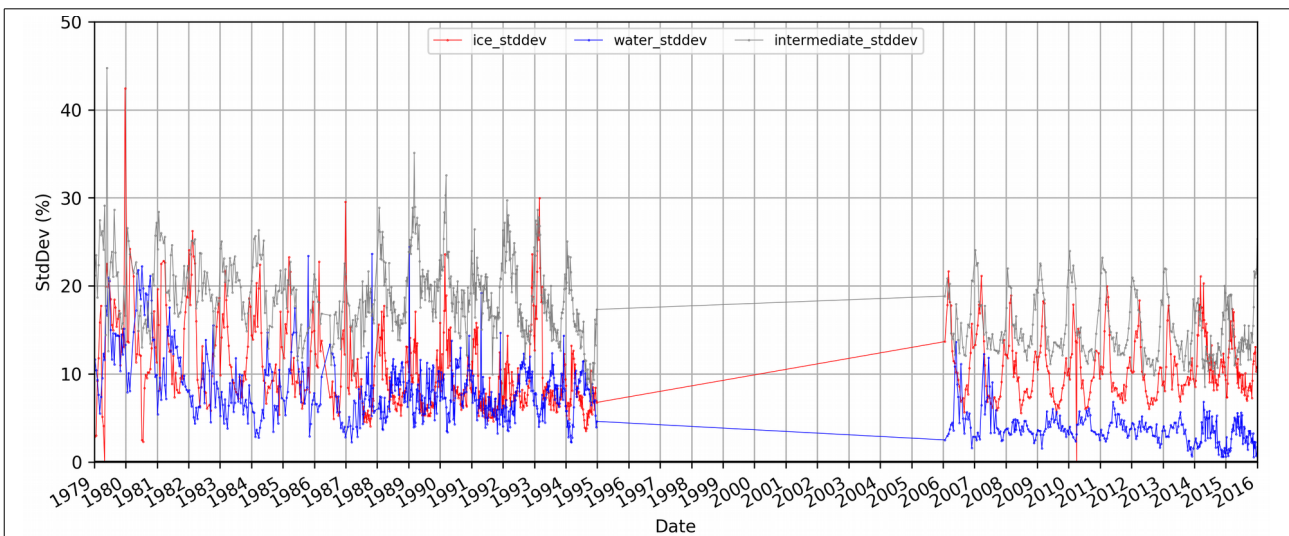


Figure 10: Southern Hemisphere standard deviation between OSI-450 and NIC ice charts: where NIC shows close ice (>99% ice), where NIC shows open water (0% ice) and where NIC shows intermediate ice concentrations (0%<SIC<=99%).

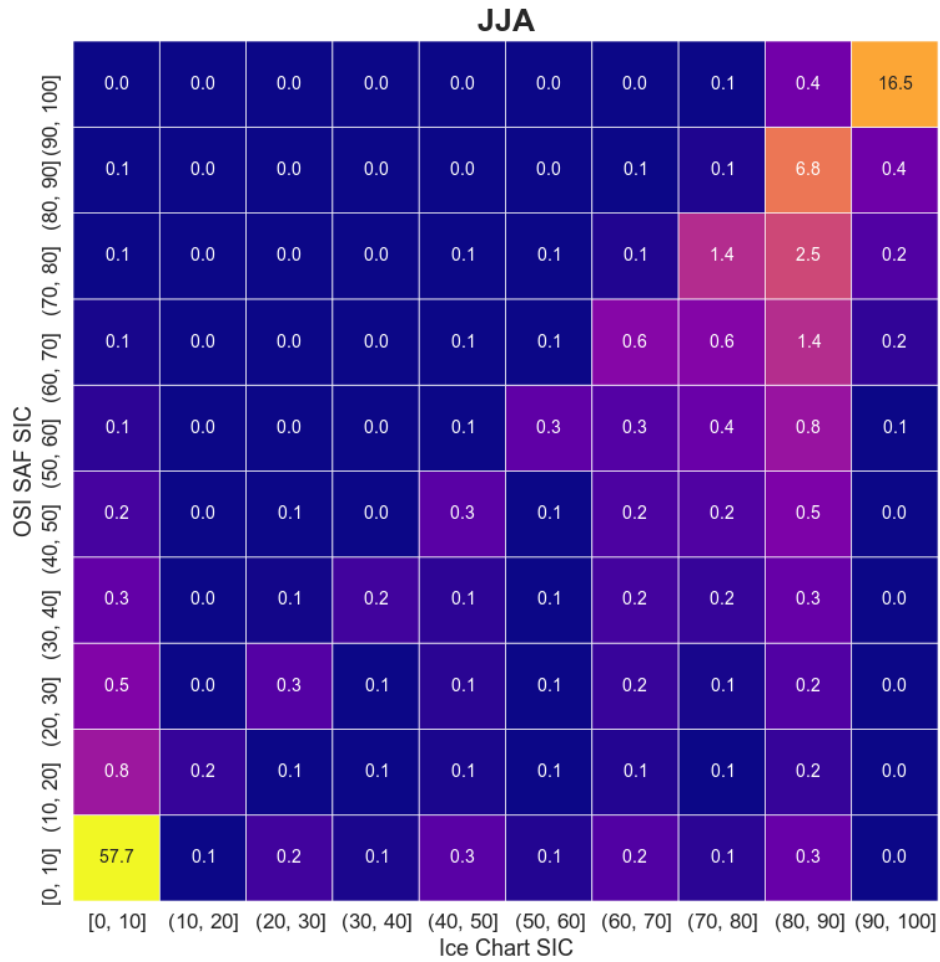


Figure 11: Density scatter plot of all corresponding OSI-450 and NIC ice chart ice concentrations in the grid point comparison. For Antarctic winter in June, July and August [JJA]. White numbers are the percentage of grid points per ice concentration category [in logarithmic scale] Ice concentration categories are defined by the open ('(') and closed ('[') boundaries.

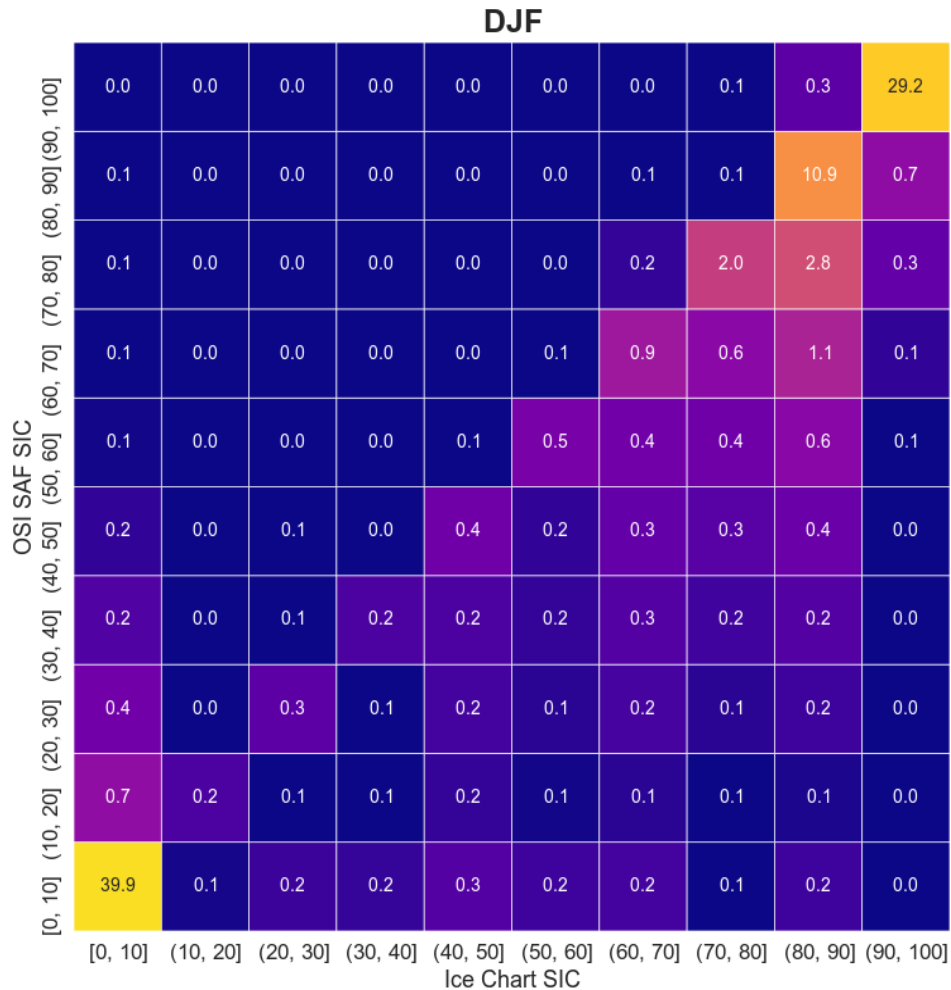


Figure 12: Density scatter plot of all corresponding OSI-450 and NIC ice chart ice concentrations in the grid point comparison. For Antarctic summer in December, January and February [DJF]. White numbers are the percentage of grid points per ice concentration category [in logarithmic scale]. Ice concentration categories are defined by the open ('(') and closed ('[') boundaries.

Sea Ice Concentration (OSI SAF vs NIC) Comparison
JJA

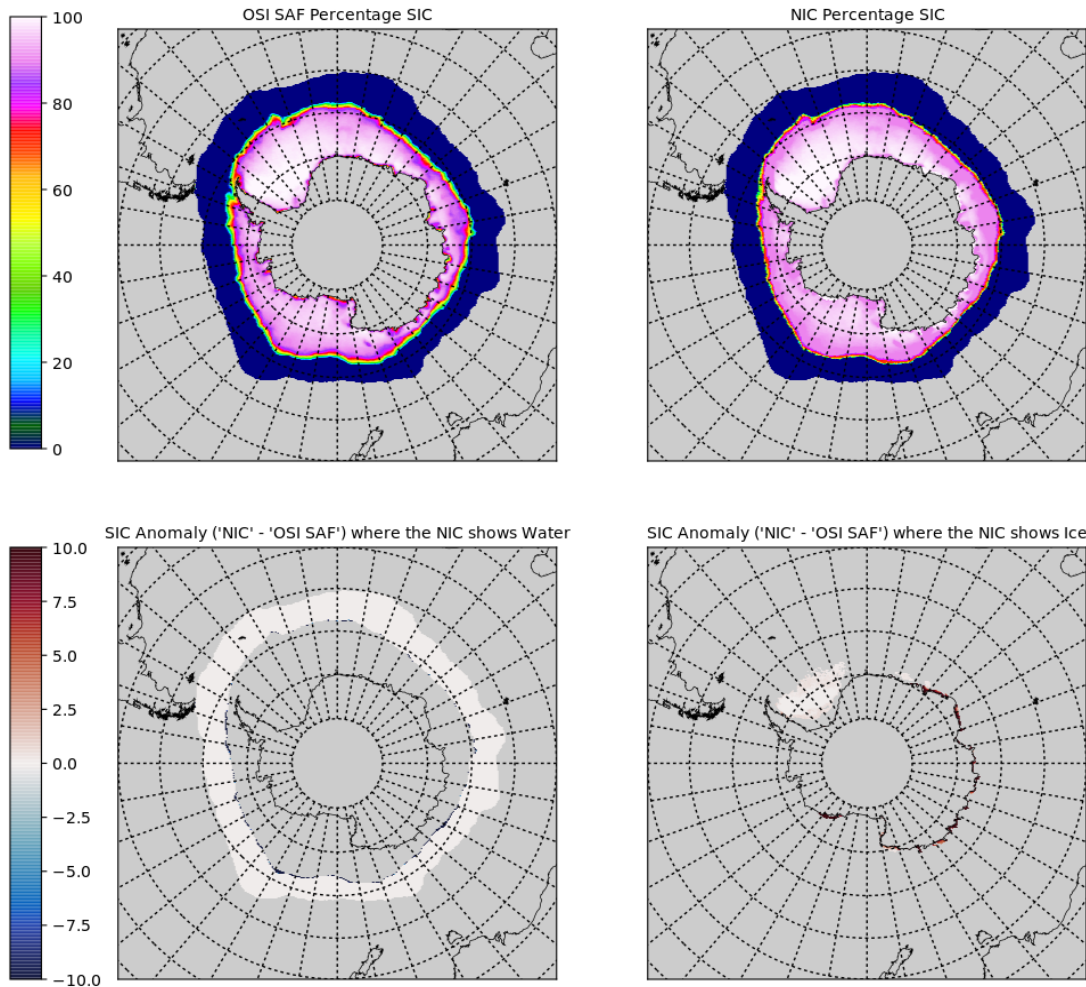


Figure 13: Map of Antarctic winter (June, July and August) median ice concentration of OSI-450 [top left] and of NIC ice charts [top right]. [bottom left] and [bottom right] show the ice concentration difference of OSI-450, where NIC ice concentrations are 0% ice and >99% ice, respectively.

Sea Ice Concentration (OSI SAF vs NIC) Comparison
DJF

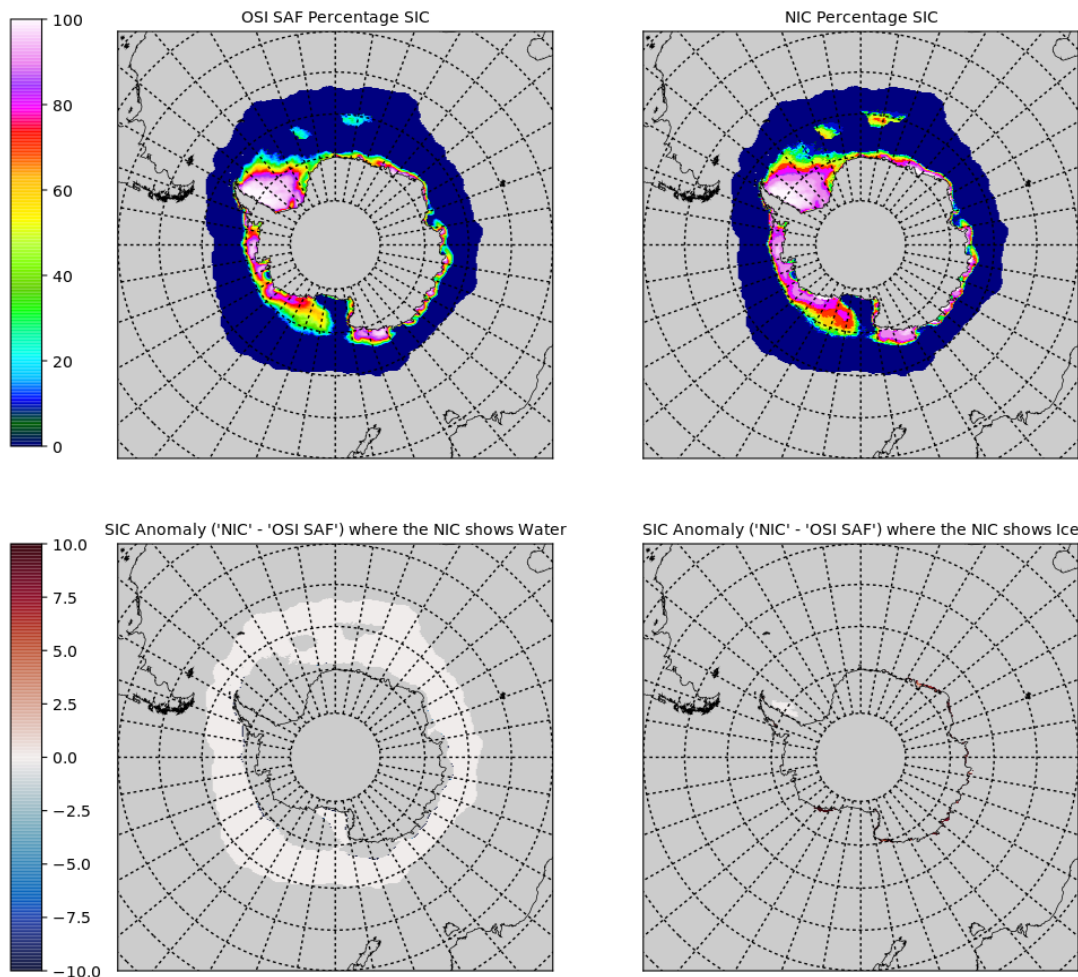


Figure 14: Map of Antarctic summer (December, January, February) median ice concentration of OSI-450 [top left] and of NIC ice charts [top right]. [bottom left] and [bottom right] show the ice concentration difference of OSI-450, where NIC ice concentrations are 0% ice and >99% ice, respectively.

2.8. Differences in validation for OSI-450 compared to OSI-409

For being able to evaluate the improved algorithm of the OSI-450 product compared to the algorithm of the prior SIC climate data record OSI-409, a comparison of the OSI-409 data record with NIC ice charts has been conducted using the same methodology as described in section 2.4 and 2.5. The validation of OSI-409 against NIC ice charts described in [RD-3] used a slightly different comparison methodology.

The general comments on the comparison figures of 'Match', 'Bias' and 'Stddev' for the OSI SAF ice concentrations (OSIC) with ice chart analysis concentrations (IAC) given in the previous section also apply for the comparison figures of the OSI-409 product and ice charts shown below. One difference is that especially the comparison results for OSI-409 for Southern Hemisphere are very noisy and a clear seasonal cycle is not evident in the first part of the comparison period up till 1995.

Figure 16, Figure 18 and Figure 20 show the difference in match, bias and standard deviation, respectively, between the OSI-409 and OSI-450 for the Northern Hemisphere. Figure 22, Figure 24 and Figure 26 show same statistics for the Southern Hemisphere.

Predominantly negative match differences in Figure 16 and Figure 22 proves that OSI-450 performs better than OSI-409 for these categories. Differences in match for Northern Hemisphere does not change much during the reanalysis period. For Southern Hemisphere, the difference in bias diminishes from late 2009 and onwards, due to an increase in the match for OSI-409. This coincides with the introduction of the OSI-409a data set in Oct. 2009. Tables of comparison statistics in 2.7.1 and 2.8.1 for Northern Hemisphere, and 2.7.2 and 2.8.2 for Southern Hemisphere, for OSI-450 and OSI-409 respectively, show that OSI-450 perform better than OSI-409 for both match categories on both a yearly and seasonal average basis.

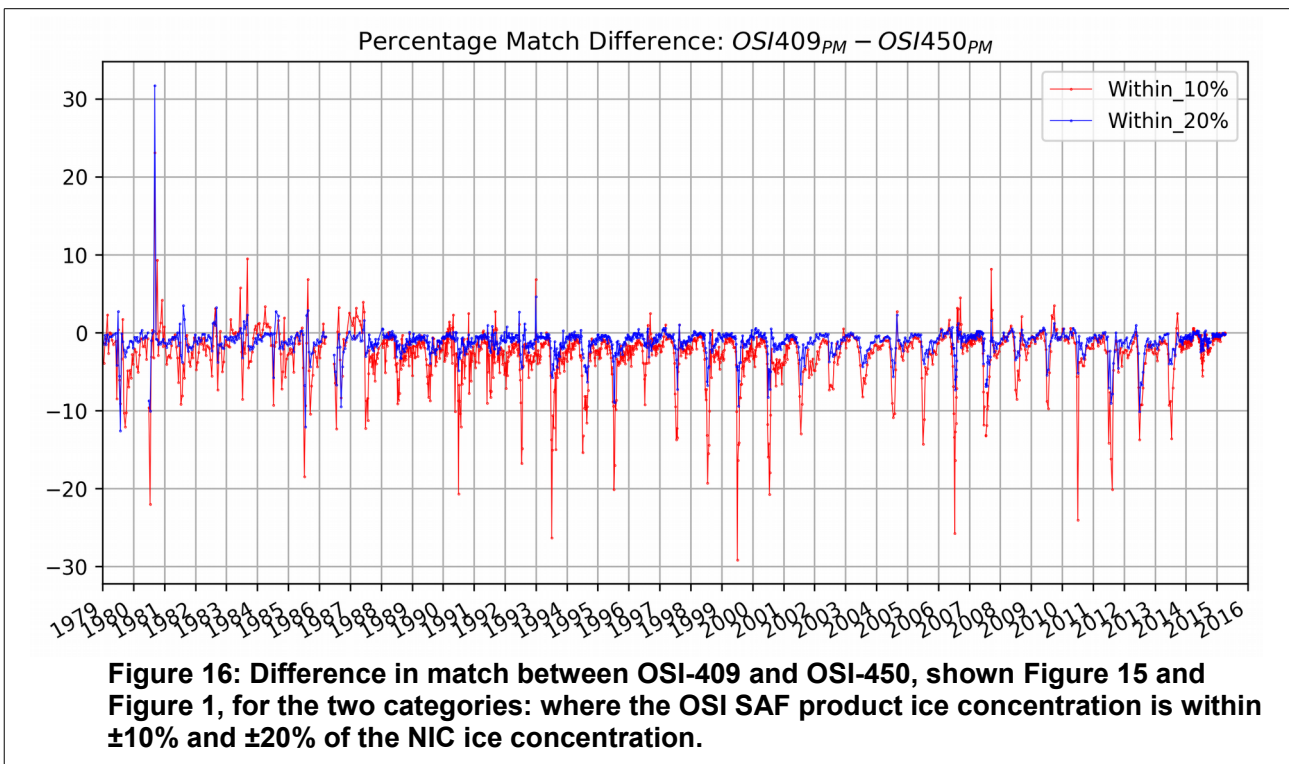
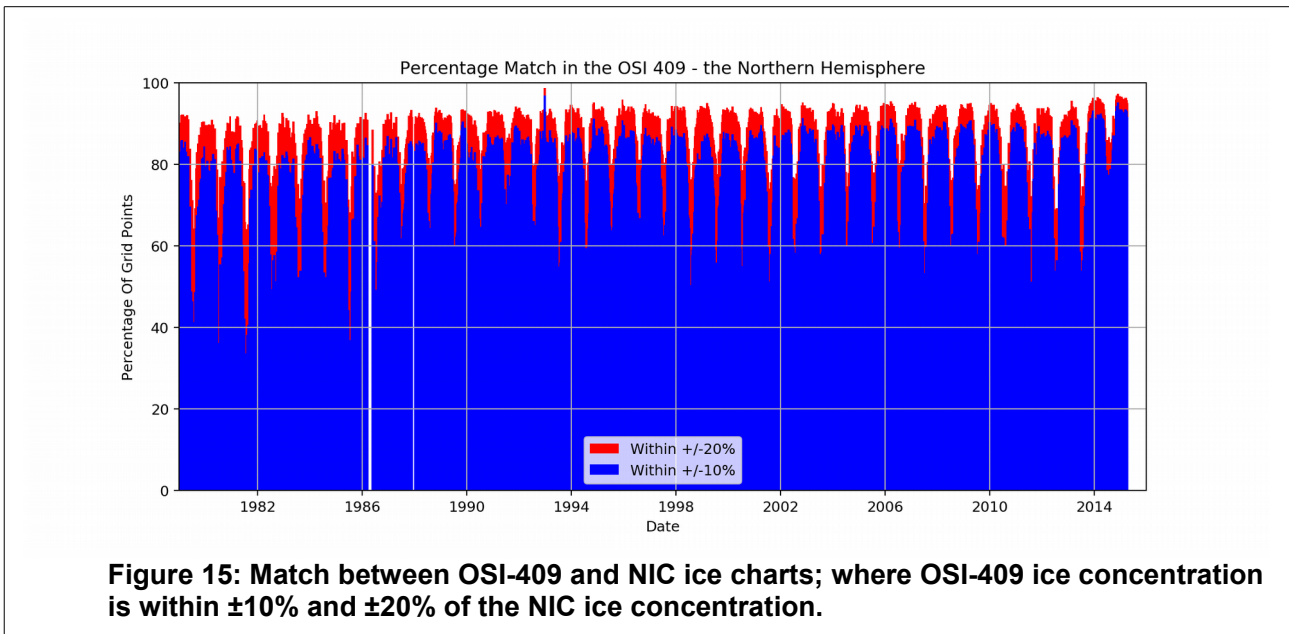
Predominantly positive ice bias and water bias differences in Figure 18 and Figure 24 proves that OSI-450 generally performs better than OSI-409 for these two categories, especially for the Northern Hemisphere. For the intermediate bias category, not much improvements are seen in the OSI-450 data set. Actually the OSI-409 performs slightly better than OSI-450, in the order of 1-2% difference on yearly average.

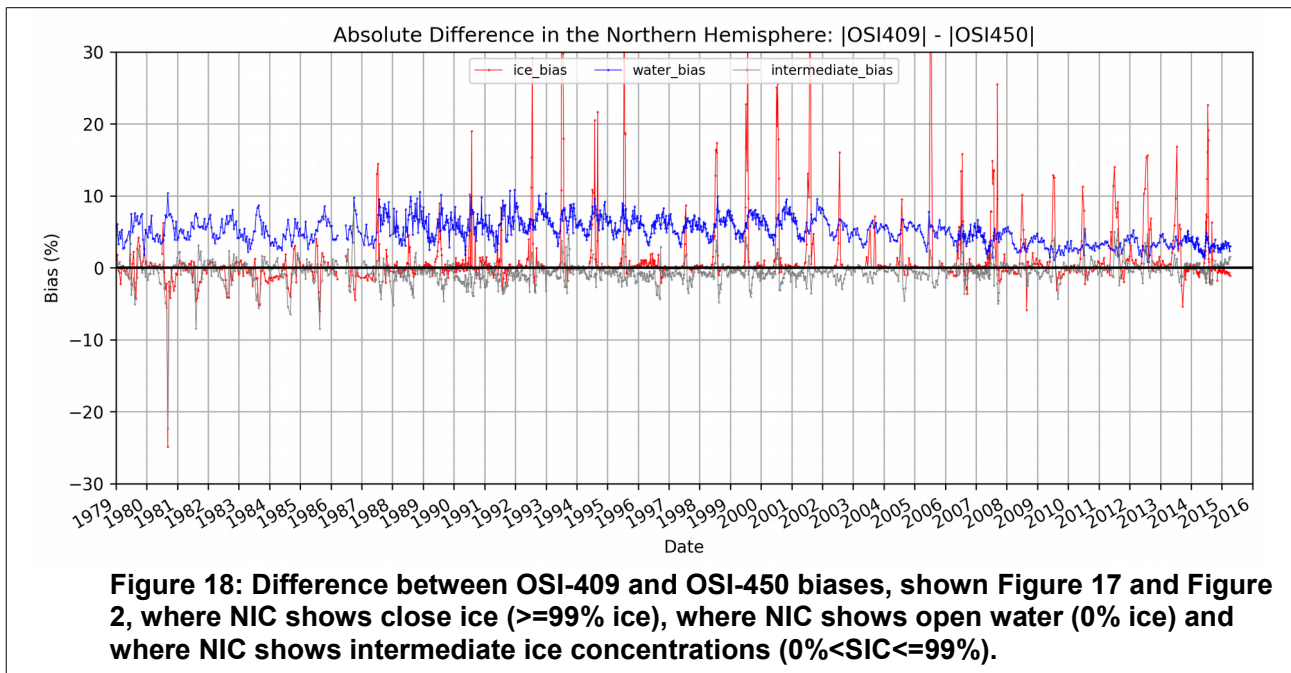
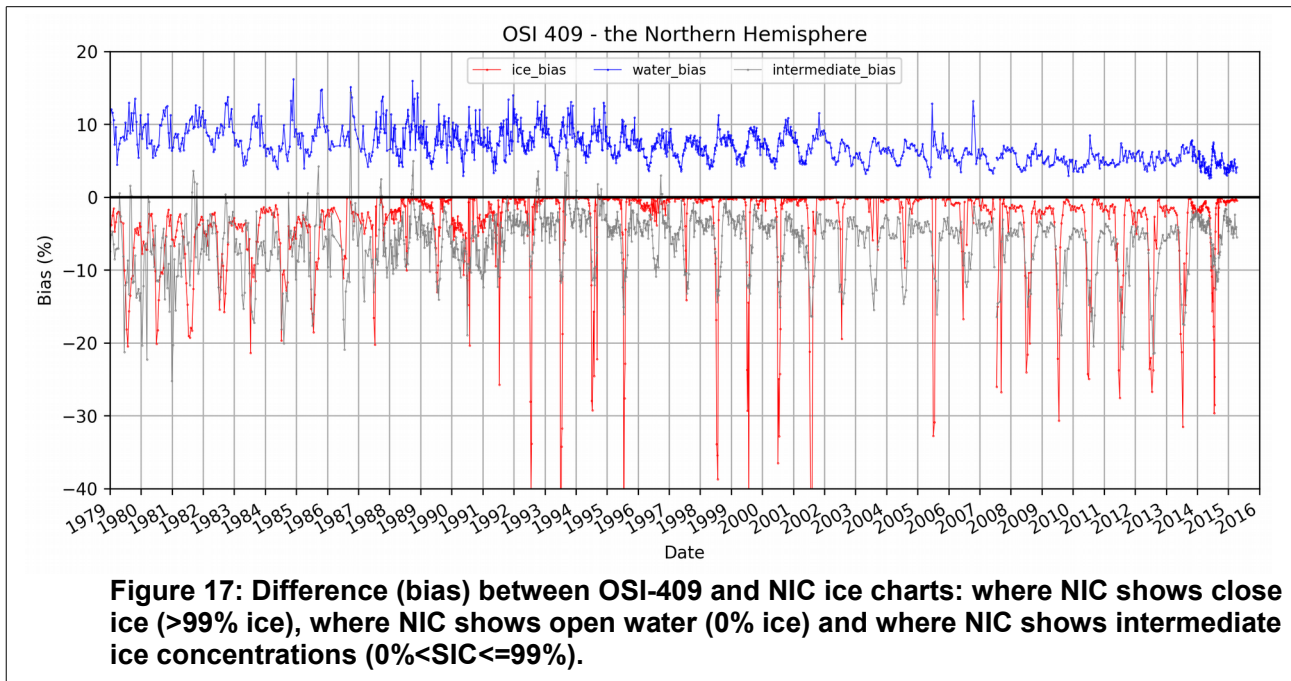
Differences in standard deviation shown in Figure 20 and Figure 26 are generally very small throughout the analysis period, at the order of +/- 1-2%. Overall, OSI-450 performs slightly better than the OSI-409 for the water category, especially for the Southern Hemisphere where this applies to both yearly and seasonal averages. However, OSI-409 performs slightly better than OSI-450 for the ice and intermediate categories, especially in the summer season and for the Northern Hemisphere. The ice standard deviation is generally lower before 2006 and there is a large reduction in the standard deviation of OSI-450 compared to -409 from 1998 to 2008 during the summer. After 2006, the water standard deviation of the OSI-450 increases a few percent in the summer compared to the OSI-409.

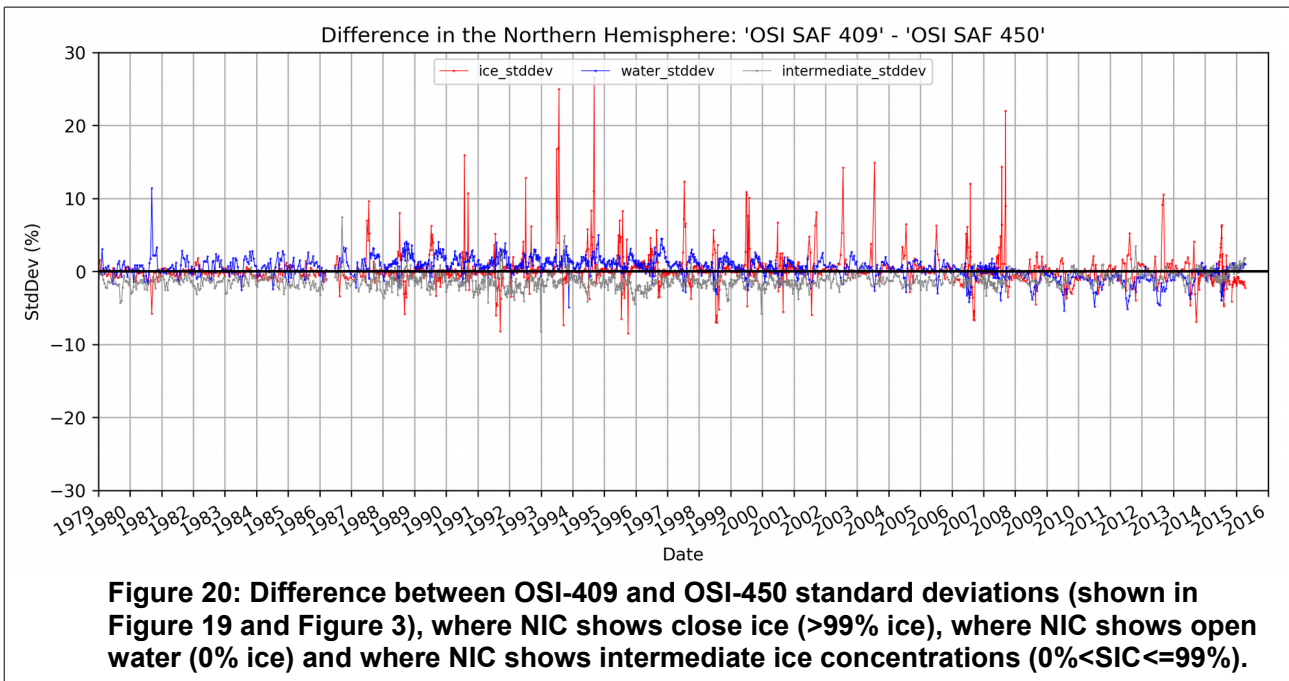
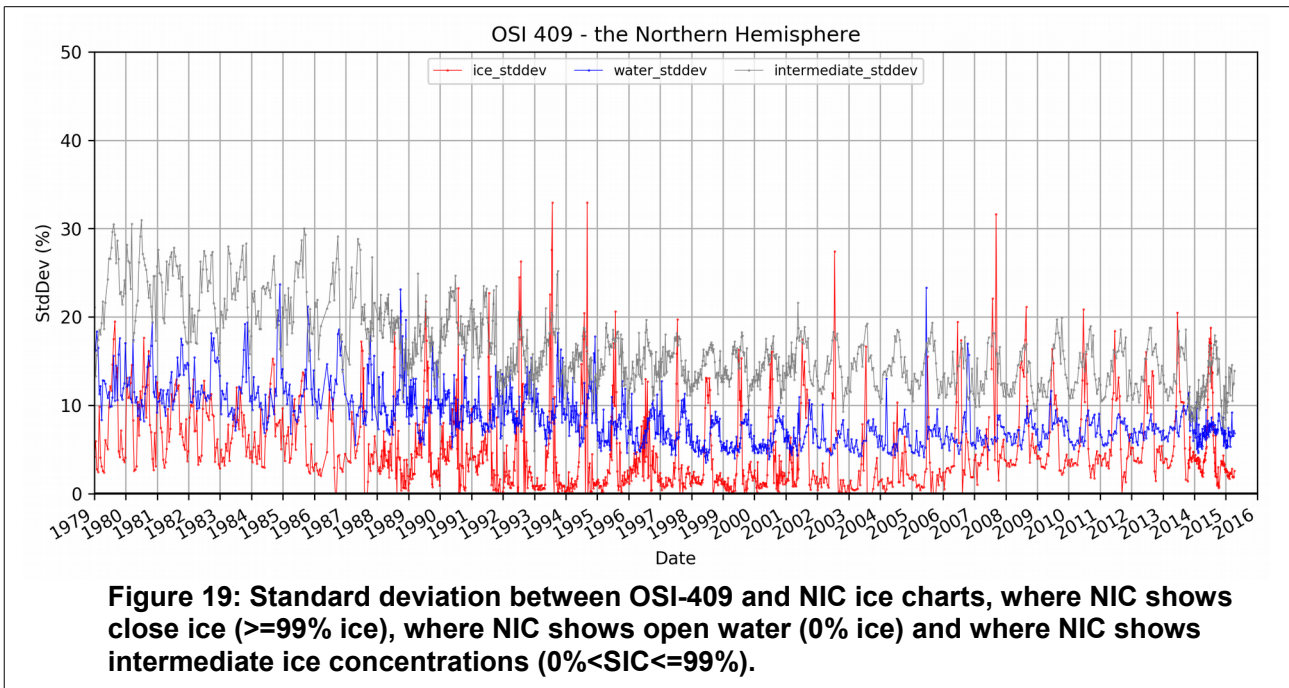
2.8.1. Northern Hemisphere

Figure 15 of percentage match shows a clear seasonal cycle with 80% to 95% of cases meeting the criteria during winter and 40% to 70% during the peak of summer melt. On average through the analysis period, 79% of the OSIC are within $\pm 10\%$ of the IAC and 88% lie within $\pm 20\%$. The difference (bias) in ice concentration in Figure 17 shows a positive water_bias at an average level of 7% through the reanalysis period. The interannual average bias for ice (100% IAC) and intermediate ice ($0\% < \text{IAC} \leq 99\%$) is -3% and -6%, respectively. Figure 19 shows the standard deviation on the ice concentration differences. Average standard deviation for the whole reanalysis period is 5% for close ice (100% IAC), 16% for intermediate ice concentrations and 8% for open water (0% IAC). Yearly average and seasonal statistics (Dec.-Feb., Jun.-Aug., Mar.-May., Sep.-Nov.) are given in the table below. Underlined numbers are where OSI-409 perform better than OSI-450:

OSI-409 NH	Match [%]		Bias [%]			Stddev [%]		
	within 10pct	within 20pct	ice	water	intermediate	ice	water	intermediate
Yearly average	79	88	-3	7	<u>-6</u>	5	8	<u>16</u>
DJF	86	93	-1	7	-5	3	8	<u>14</u>
JJA	63	80	-9	7	<u>-10</u>	10	8	<u>18</u>
MAM	85	92	-1	5	-5	<u>3</u>	7	<u>16</u>
SON	81	89	-2	8	<u>-4</u>	<u>3</u>	10	16





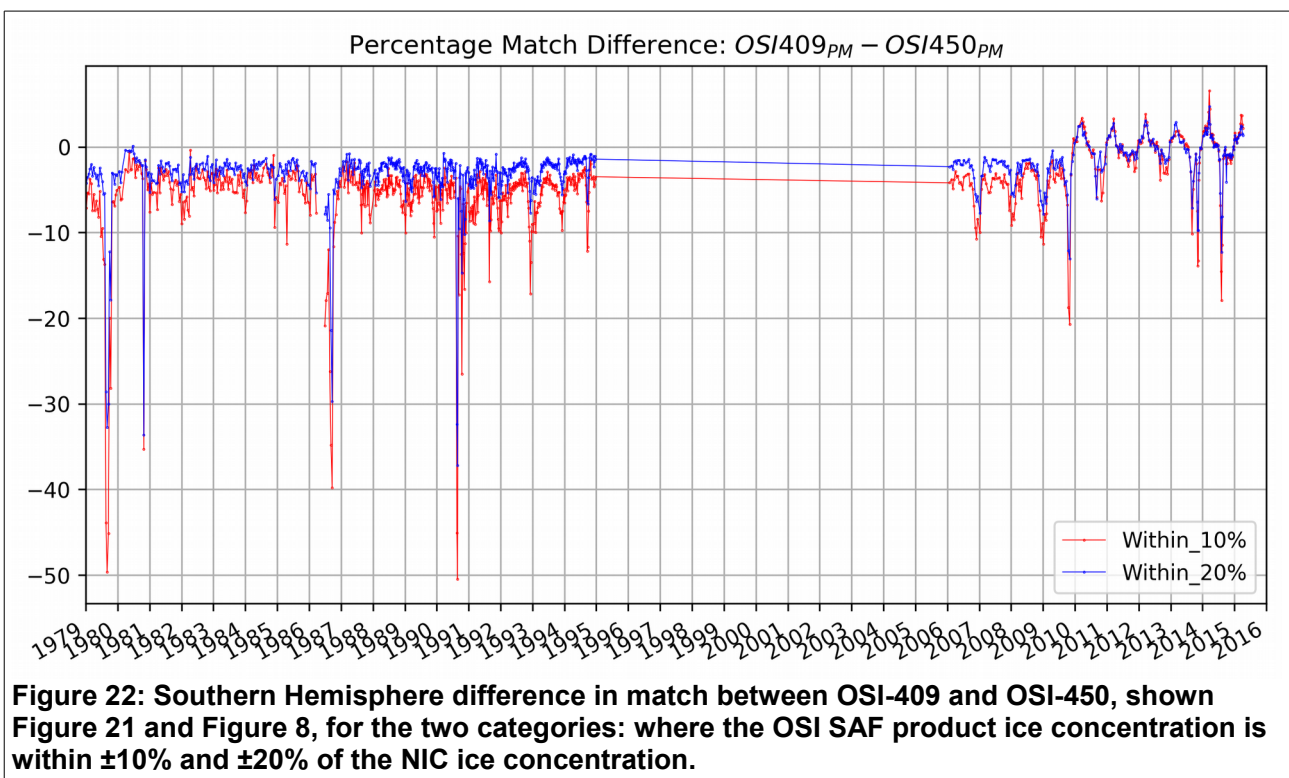
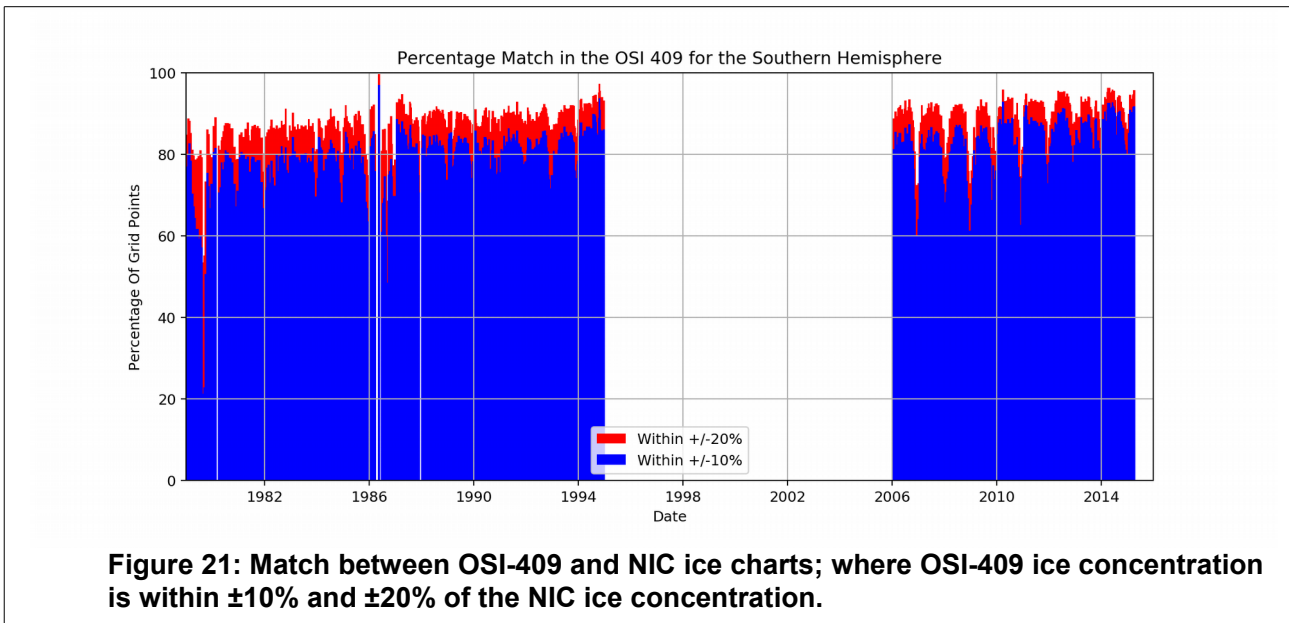


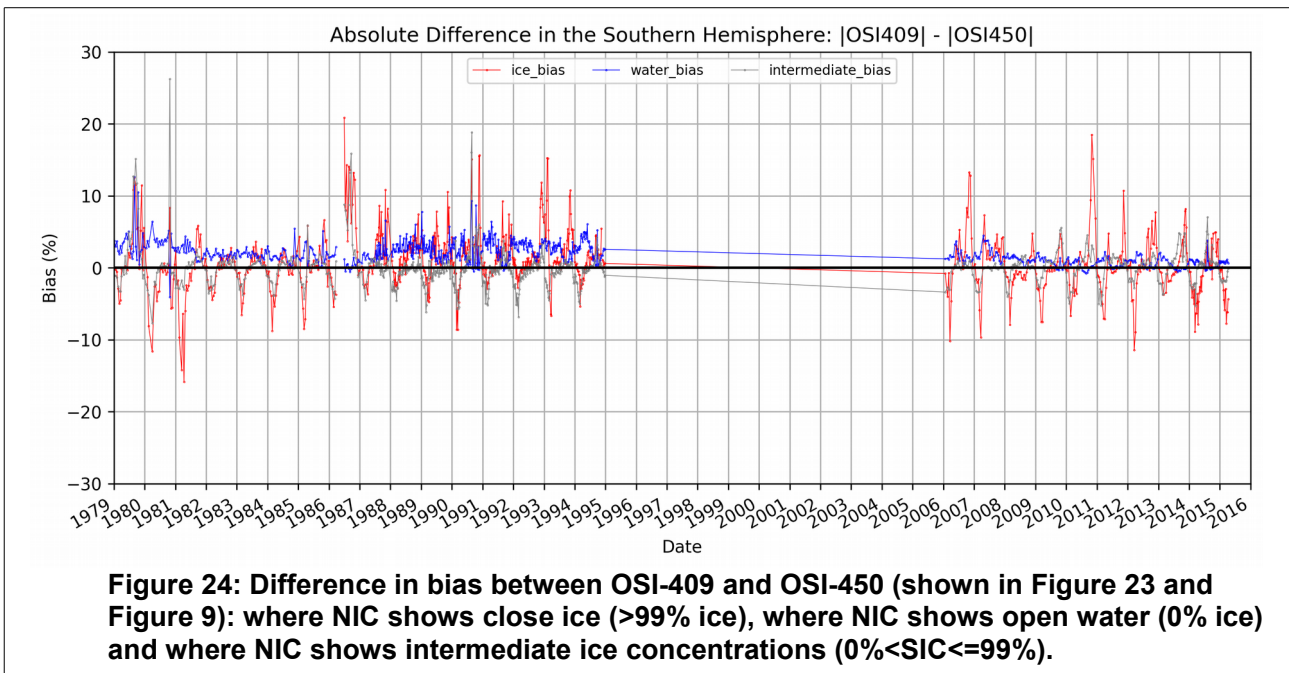
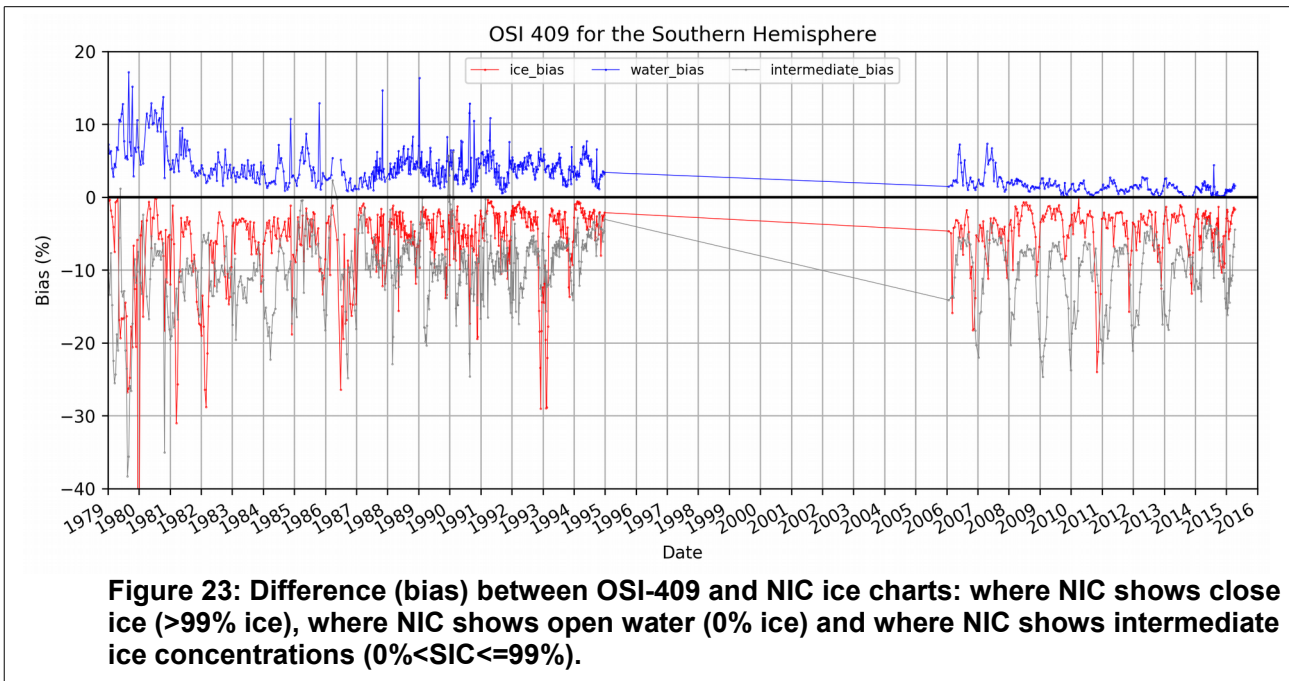
2.8.2. Southern Hemisphere

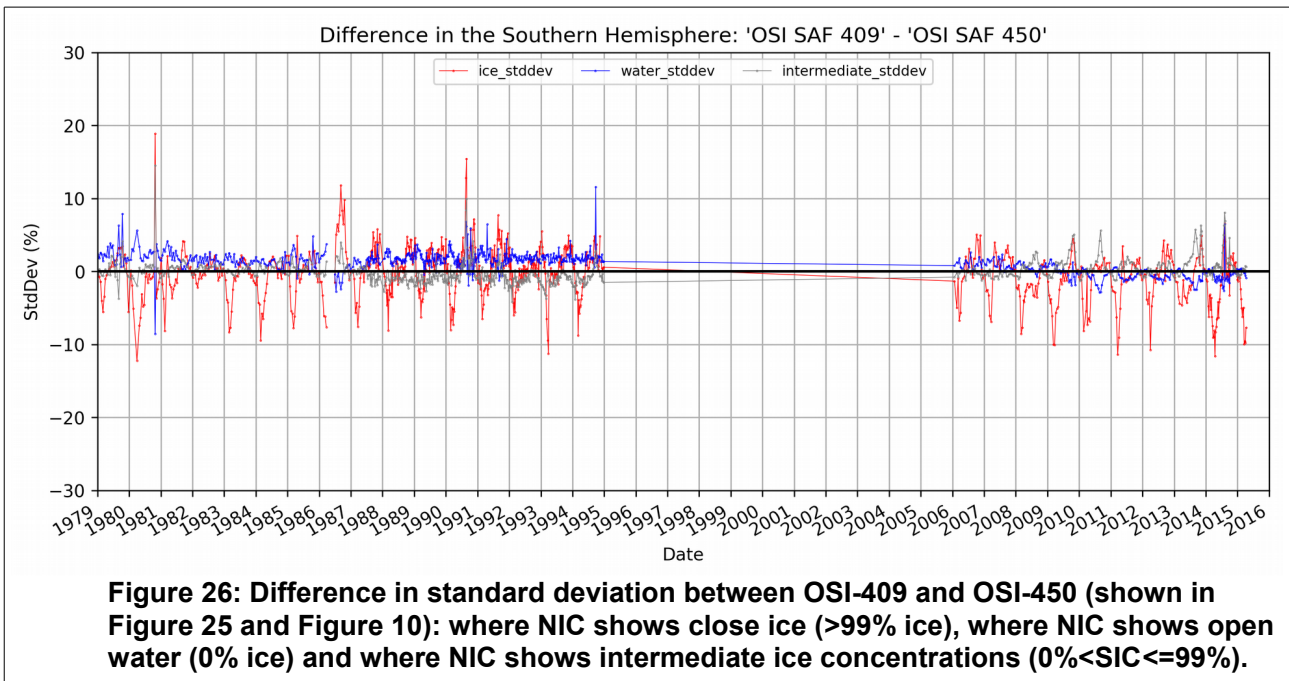
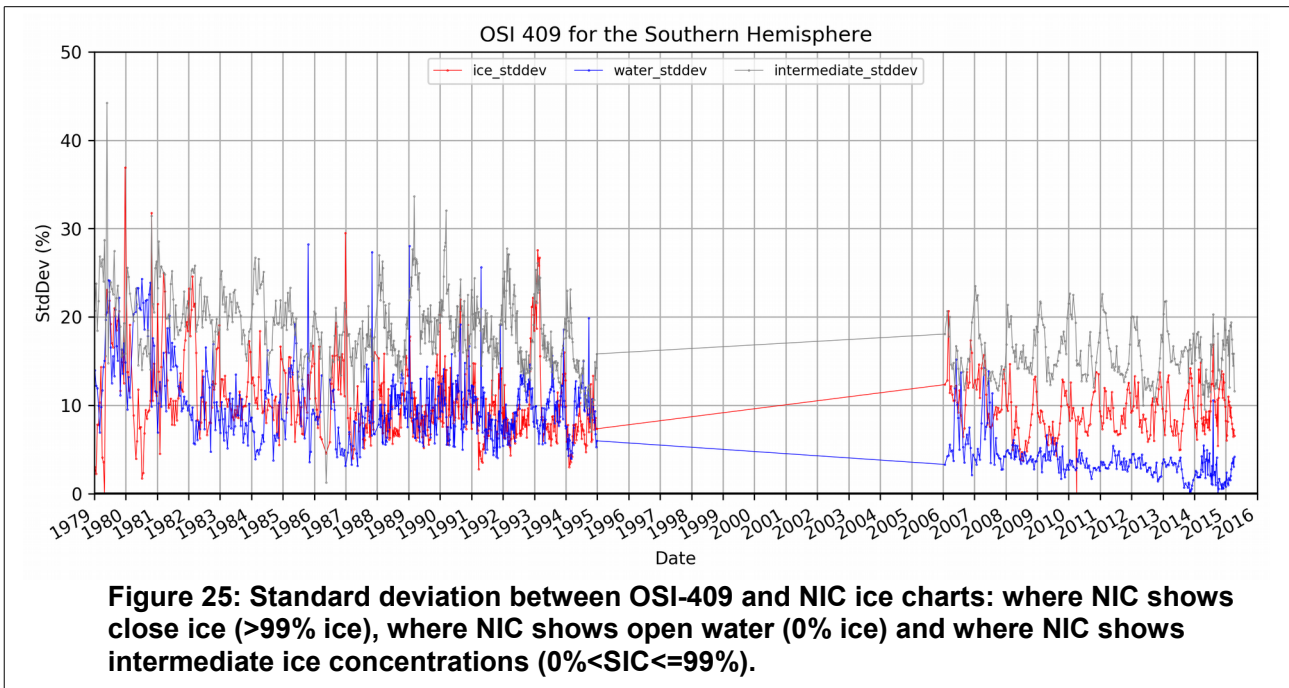
Figure 21 shows the percentage match between data sets with a clear seasonal cycle of 60% to 95% of cases meeting the criteria during Antarctic winter and 60% to 80% during the peak of summer melt. On average through the analysis period, 80% of the OSIC are within $\pm 10\%$ of the IAC and 88% lie within $\pm 20\%$. The difference (bias) in ice concentration in Figure 23 shows a positive water_bias at an average level of 3% through the reanalysis period. The interannual average bias for ice (100% IAC) and intermediate ice is -6% and -10%, respectively. Figure 25 shows the standard deviation on the ice concentration differences. Yearly average standard deviation for the whole reanalysis period is 10% for close ice, 18% for intermediate ice concentrations ($0\% < \text{IAC} \leq 99\%$) and 8% for open water (0% IAC).

Yearly average and seasonal statistics (Dec.-Feb., Jun.-Aug., Mar.-May., Sep.-Nov.) are given in the table below. Underlined numbers are where OSI-409 perform better than OSI-450:

OSI-409 SH	Match [%]		Bias [%]			Stddev [%]		
	within 10pct	within 20pct	ice	water	intermediate	ice	water	intermediate
Yearly average	80	88	-6	3	-10	10	8	18
DJF	77	85	-6	3	<u>-12</u>	<u>12</u>	7	<u>20</u>
JJA	82	89	-5	4	-8	9	10	16
MAM	81	89	<u>-4</u>	4	<u>-10</u>	9	8	19
SON	78	87	-7	3	-9	11	8	16







2.9. Comparison between the OSI-430-b and NIC ice charts

Comparisons between National Ice Center (NIC) ice charts and the OSI SAF OSI-430-b sea ice concentration continuous reprocessing product, ICDR v.2, for Northern and Southern Hemispheres are shown in the following two sections. The OSI-430-b ICDR v.2 operationally extends the OSI-450 and replaces the OSI-430 ICDR v.1 as the continuously updated OSI SAF sea ice concentration CDR. The validation period cover 2015 to 2017. Some of the figures show additional comparison data from January to July 2018, but this partial year of 2018 is not included in the validation statistics that is reported in the tables below.

The general comments on the comparison figures of 'Match', 'Bias' and 'Stddev' for the OSI SAF ice concentrations (OSIC) with ice chart analysis concentrations (IAC) and its general seasonal behaviour given in the previous sections also apply for the comparison figures of the OSI-430-b product and ice charts shown below.

2.9.1. Northern Hemisphere

The percentage match in Figure 27 shows a clear seasonal cycle with 90% to 95% of cases meeting the criteria during winter and 70% to 80% during the peak of summer melt. On average through the analysis period, 87% of the OSIC are within $\pm 10\%$ of the IAC and 91% lie within $\pm 20\%$. The difference (bias) in ice concentration in Figure 28 shows a positive water_bias at an average level of 2% through the analysis period. The interannual average bias for ice (>99% IAC) is -3%. The ice bias experiences some fluctuations during summer melt season. Figure 29 shows the standard deviation on the difference (bias) in ice concentrations given in Figure 28. The yearly average standard deviation for the whole reanalysis period is 7% for close ice (>99% IAC) and 9% for open water (0% IAC). Yearly average and seasonal statistics (Dec.-Feb., Jun.-Aug., Mar.-May., Sep.-Nov.) are given in the table below:

OSI-430-b NH	Match [%]		Bias [%]			Stddev [%]		
	within 10pct	within 20pct	ice	water	Intermediate ice	ice	water	Intermediate ice
2015 - 2017								
yearly average	87	91	-3	2	-6	7	9	14
DJF	92	95	-2	1	-3	4	7	11
MAM	91	94	-2	1	-4	5	7	13
JJA	76	84	-9	3	-11	13	10	17
SON	88	92	-2	3	-5	5	10	13

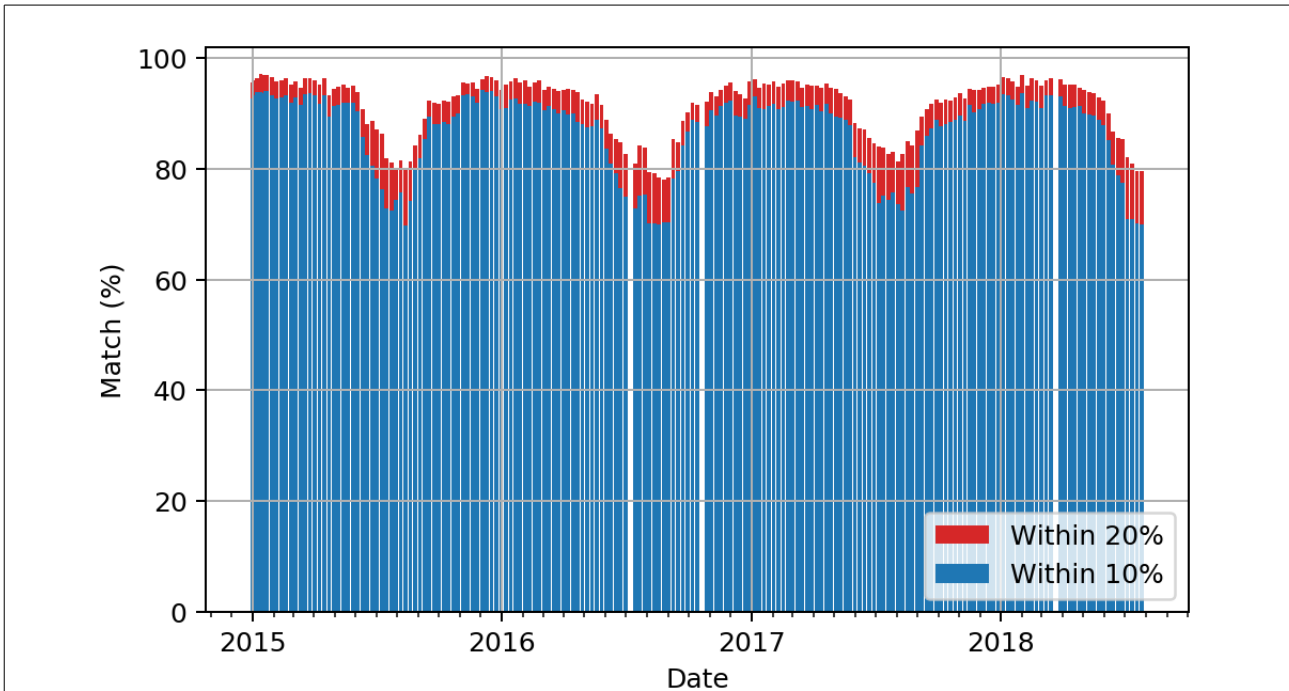


Figure 27: Match between OSI-430-b and NIC ice charts; where OSIC is within $\pm 10\%$ and $\pm 20\%$ of the NIC ice concentration.

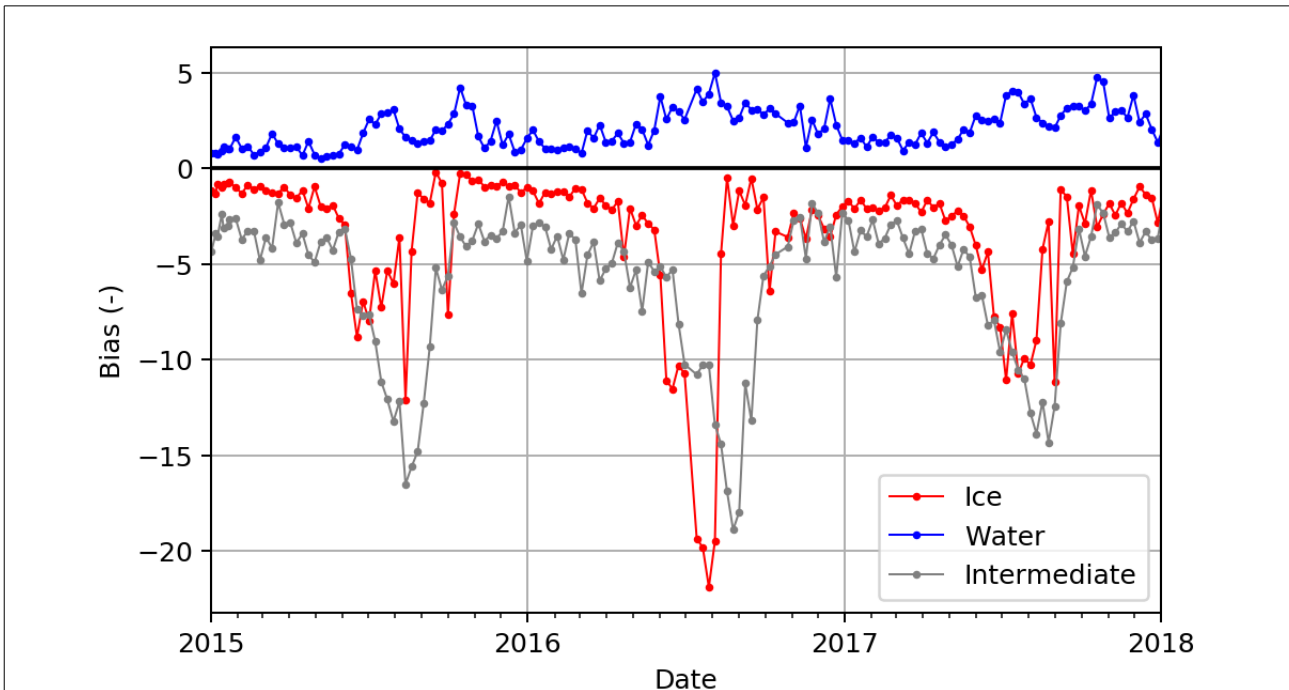


Figure 28: Difference (bias) between OSI-430-b and NIC ice charts: where NIC shows ice ($>99\%$ ice), intermediate ($99\% < \text{ice} > 0\%$) and water (0% ice).

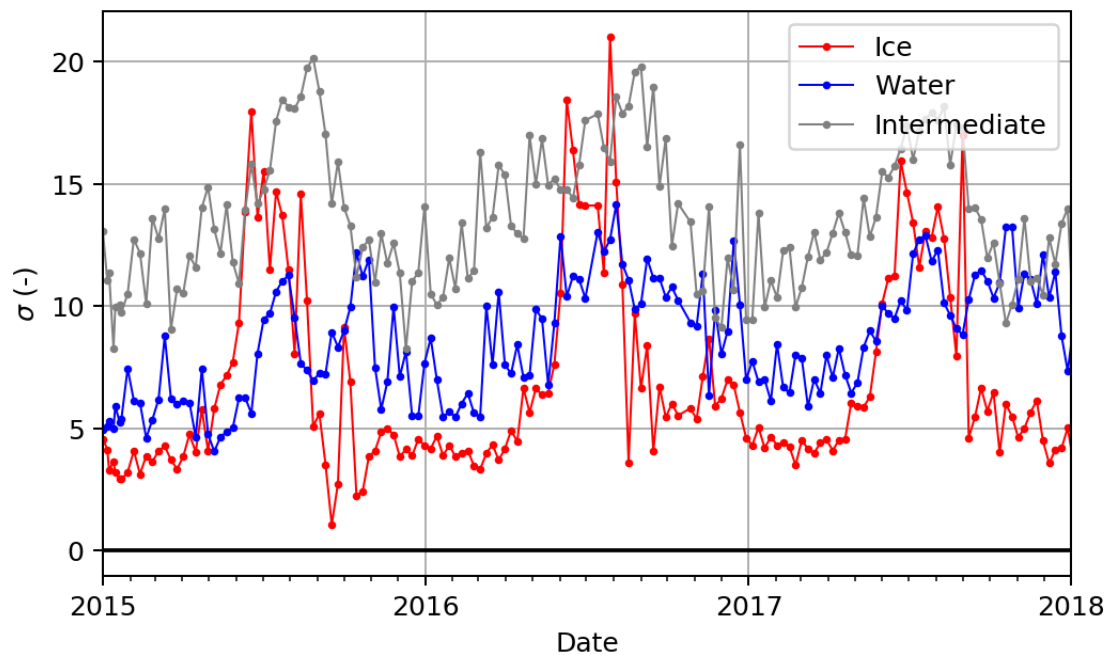


Figure 29: Standard deviation between OSI-430-b and NIC ice charts: where NIC shows ice (>99% ice), intermediate (99% < ice > 0%) and water (0% ice).

2.9.2. Southern Hemisphere

The percentage match in Figure 30 shows a clear seasonal cycle with 90% to 95% of cases meeting the criteria during winter and 70% to 80% during the peak of summer melt. On average through the analysis period, 85% of the OSIC are within $\pm 10\%$ of the IAC and 91% lie within $\pm 20\%$. The difference (bias) in ice concentration in Figure 31 shows that there is close to zero bias for the open water category through the three-year period. The average bias for ice (>99% IAC) is -8%. The ice bias experience some fluctuations over the three-year period, but without a clear cycle. Two cases of very high ice biases are seen in Antarctic Fall on April 21st 2016 and May 6th 2016, due to sudden decrease in OSI-430-b ice concentrations. These events are possibly linked to the extreme low ice extent in Antarctic summer 2016 that lasted until start of April and thus could have had an effect on the computation of the OSI-430-b dynamical tie-points (which are calculated differently than for OSI-430). Figure 32 show the standard deviation on the difference (bias) in ice concentrations given in Figure 33. The yearly average standard deviation for the whole three-year period is 11% for close ice (>99% IAC) and 3% for open water (0% IAC). Yearly average and seasonal statistics (Dec.-Feb., Jun.-Aug., Mar.-May., Sep.-Nov.) are given in the table below:

OSI-430-b SH	Match [%]		Bias [%]			Stddev [%]		
	within 10pct	within 20pct	ice	water	Intermediate ice	ice	water	Intermediate ice
2015 - 2017								
yearly average	85	91	-8	0	-11	11	3	17
DJF	84	88	-8	0	-18	14	2	21
MAM	89	94	-9	1	-8	14	4	15
JJA	87	94	-6	1	-6	8	5	16
SON	80	90	-8	0	-11	10	3	17

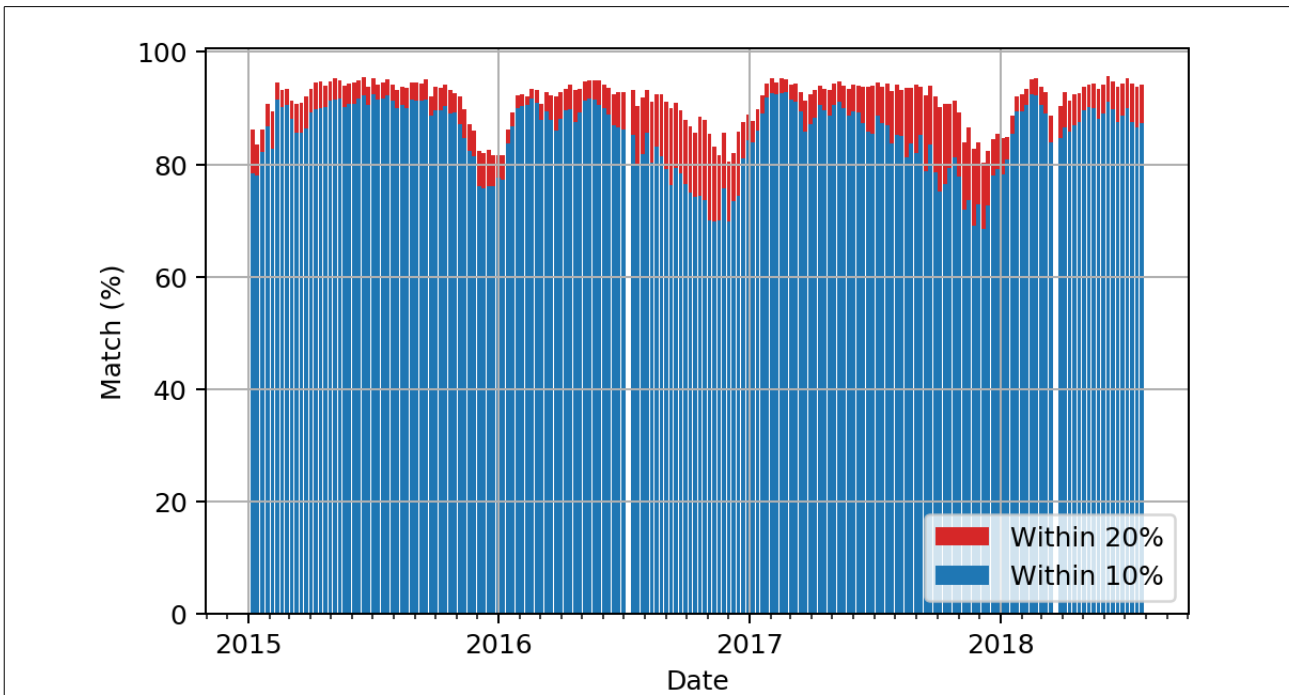


Figure 30: Southern Hemisphere match between OSI-430-b and NIC ice charts; where OSI-430-b ice concentration is within $\pm 10\%$ and $\pm 20\%$ of the NIC ice concentration.

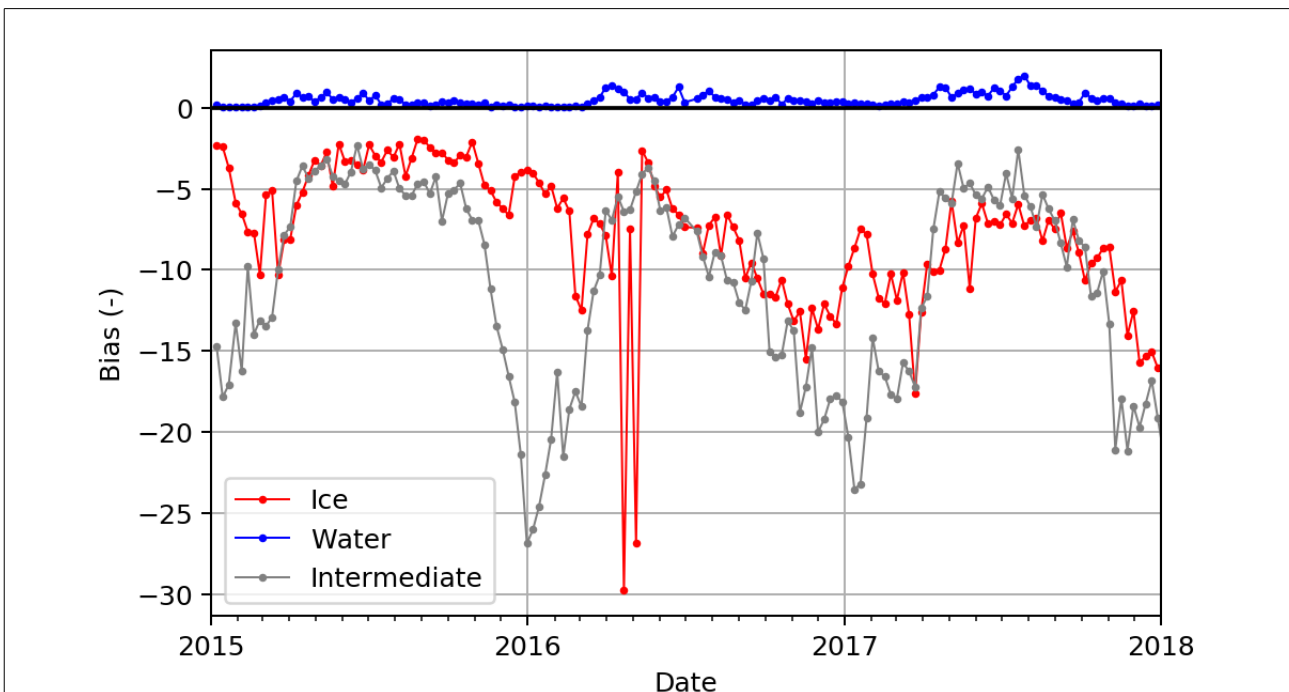


Figure 31: Southern Hemisphere difference (bias) between OSI-430-b and NIC ice charts: where NIC shows ice (>99% ice), intermediate (99% < ice > 0%) and water (0% ice).

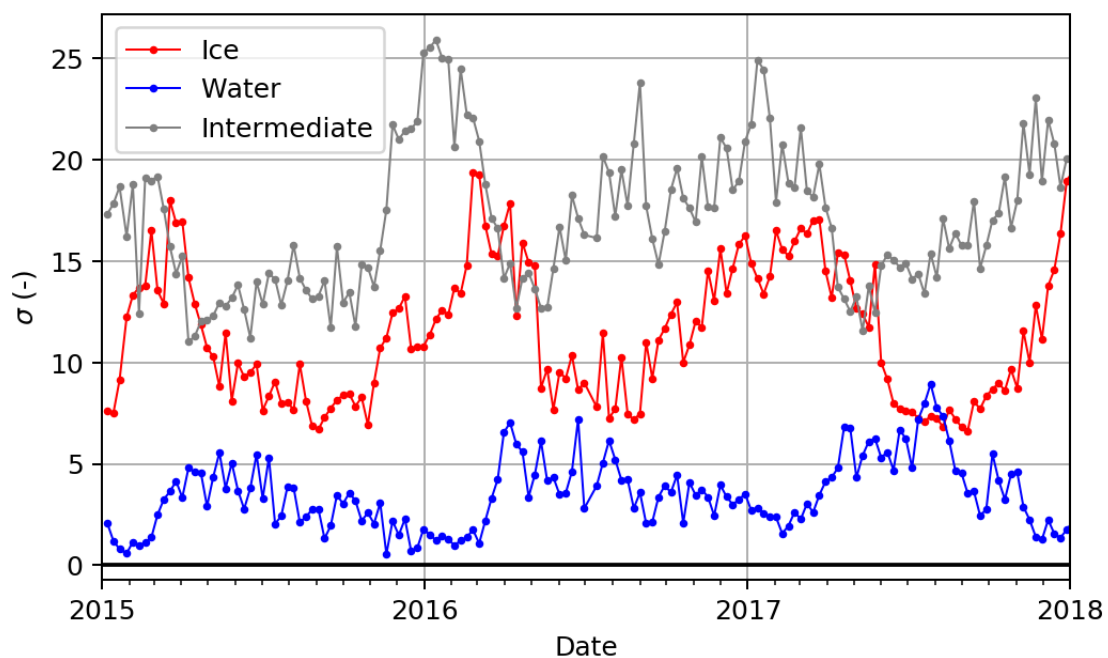


Figure 32: Southern Hemisphere standard deviation between OSI-430-b and NIC ice charts: where NIC shows ice (>99% ice), intermediate (99%< ice >0%) and water (0% ice).

2.10. Differences in validation for OSI-430-b compared to OSI-450 and OSI-430

The validation results of the OSI-430-b ICDR are here compared to those of the OSI-450 CDR in the overlapping year of 2015 to show the temporal consistency between the CDR and the ICDR products. Validation statistics for OSI-450 in 2015 are shown in the figures in chapter 2.7 and thus these graphs are not reproduced below.

Moreover, the OSI-430-b validation results are compared to those of its predecessor, the OSI-430 ICDR v.1, in the overlapping years 2016-2017 to show its relative improvements. OSI-430 validation statistics are shown in graphs on figures 33 to 38 below. The figures show additional comparison data from 2018 and beginning of January 2019, but these data are not included in the validation statistics that is reported in the tables below.

The validation statistics of OSI-450 and OSI-430 shown below are conducted using the same methodology of comparing the OSI SAF products with NIC ice charts, as described in section 2.4 and 2.5.

2.10.1. Northern Hemisphere

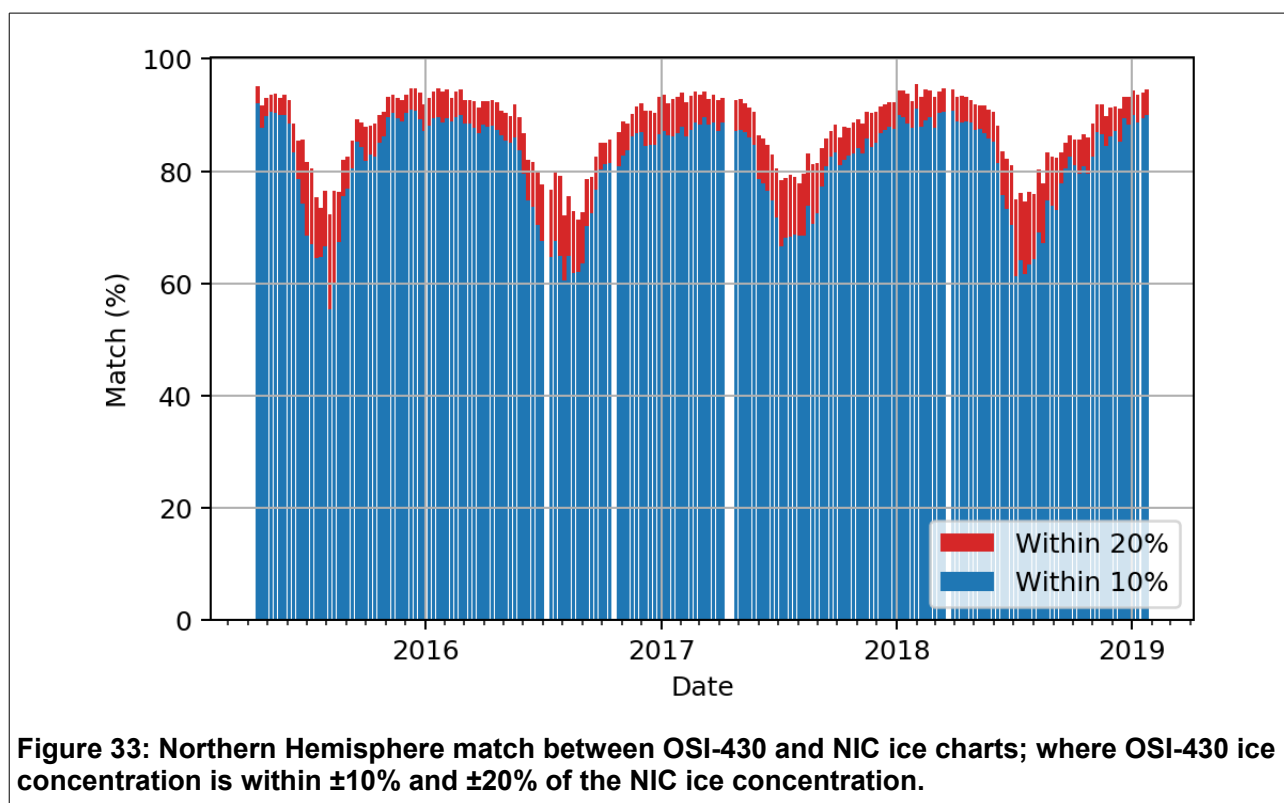
Yearly average statistics are given in the table below for the overlapping years of the comparison of OSI-430-b with OSI-450 (in 2015) and OSI-430 (through 2016-2017), respectively. Underlined numbers are where OSI-430-b perform better than OSI-450 and/or OSI-430.

It is shown that the OSI-430-b performs equally good as the OSI-450 when comparing the yearly average validation statistics (for all statistical parameters the differences are on the first decimal).

When comparing OSI-430-b to the OSI-430, it is clear from the validation statistics that the new ICDR performs better than its predecessor for the Northern Hemisphere. Especially the biases on the ice and water categories have decreased somewhat in OSI-430-b, compared to OSI-430. When comparing seasonal statistics for the ice category, it is found that OSI-430-b and OSI-430 have comparable performances in winter, with some interannual differences. In Spring and Summer (May to September) OSI-430-b has both a much smaller bias and standard deviations on the bias. Maps (not shown in this report) of Summer season ice concentrations differences between OSI-430-b and OSI-430 against ice charts, respectively, suggests that OSI-430-b is better at resolving ice concentrations in the coastal regions. For the water category the OSI-430-b has lower bias and standard deviations all-year round and especially in Winter and Spring (December – May).

NH	Match [%]		Bias [%]			Stddev [%]		
	within 10pct	within 20pct	ice	water	Intermediate ice	ice	water	Intermediate ice
2015 yearly average								
OSI-430-b	88	92	-2	2	-5	6	7	13
OSI-450	88	92	-2	2	-5	6	7	13

NH	Match [%]		Bias [%]			Stddev [%]		
	within 10pct	within 20pct	ice	water	Intermediate ice	ice	water	Intermediate ice
2016 - 2017 yearly average								
OSI-430-b	<u>86</u>	<u>91</u>	<u>-4</u>	2	<u>-6</u>	<u>7</u>	9	<u>14</u>
OSI-430	81	88	-6	8	-6	8	12	14



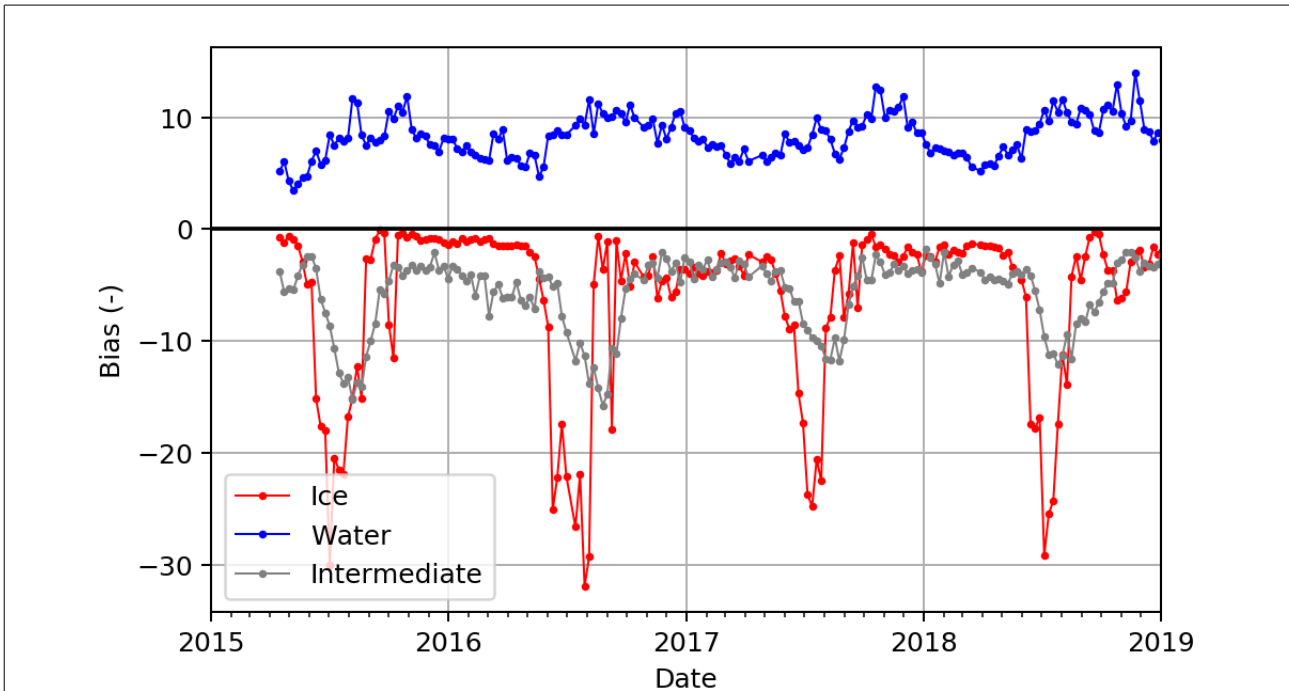


Figure 34: Northern Hemisphere difference (bias) between OSI-430 and NIC ice charts: where NIC shows ice (>99% ice), intermediate (99%< ice >0%) and water (0% ice).

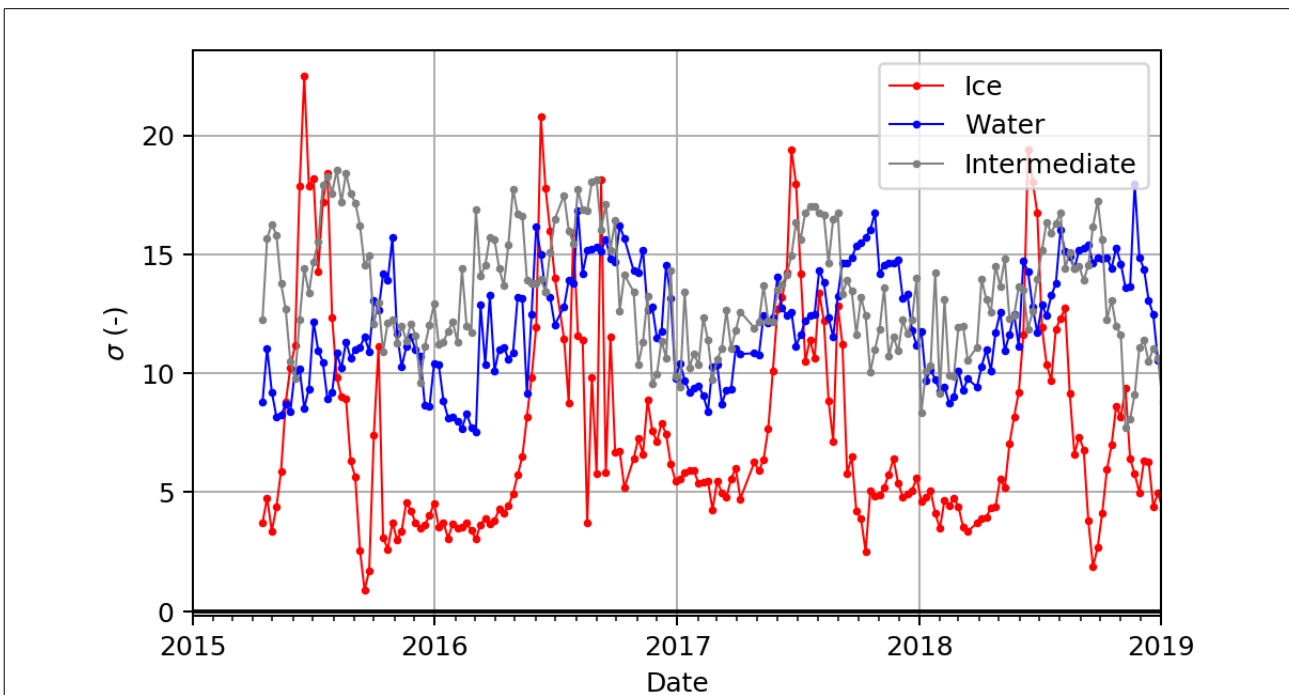


Figure 35: Northern Hemisphere standard deviation between OSI-430 and NIC ice charts: where NIC shows ice (>99% ice), intermediate (99%< ice >0%) and water (0% ice).

2.10.2. Southern Hemisphere

Yearly average statistics are given in the table below for the overlapping years of OSI-430-b with OSI-450 (in 2015) and OSI-430 (through 2015-2016), respectively. Underlined numbers are where OSI-430-b perform better than OSI-450 and/or OSI-430.

It is shown that the OSI-430-b performs equally good as the OSI-450 when comparing the yearly average validation statistics.

When comparing OSI-430-b to the OSI-430, the validation statistics show that the new ICDR overall performs better than its predecessor for the match categories. Also for the water category the new ICDR show little better results than the old ICDR and when looking at the seasonality of the water category statistics it is found that OSI-430-b especially performs better than OSI-430 in the Spring and Summer months (November – March). For the ice category, the 2016-2017 yearly average bias and standard deviation on the bias have increased with the OSI-430-b, compared to the OSI-430. Comparing the OSI-430-b and OSI-430 seasonal statistics (only shown here in graphs) it shows that OSI-430-b perform best in Winter and Spring (July to December) and perform worse in Summer/Fall (January to April).

SH	Match [%]		Bias [%]			Stddev [%]		
	within 10pct	within 20pct	ice	water	Intermediate ice	ice	water	Intermediate ice
2015 yearly average								
OSI-430-b	88	92	-4	0	-9	<u>10</u>	3	15
OSI-450	88	92	-4	0	-9	11	<u>3</u>	14

SH	Match [%]		Bias [%]			Stddev [%]		
	within 10pct	within 20pct	ice	water	Intermediate ice	ice	water	Intermediate ice
2016 - 2017 yearly average								
OSI-430-b	<u>84</u>	<u>91</u>	-9	<u>1</u>	<u>-12</u>	12	<u>4</u>	18
OSI-430	82	90	-9	1	-13	<u>10</u>	3	<u>19</u>

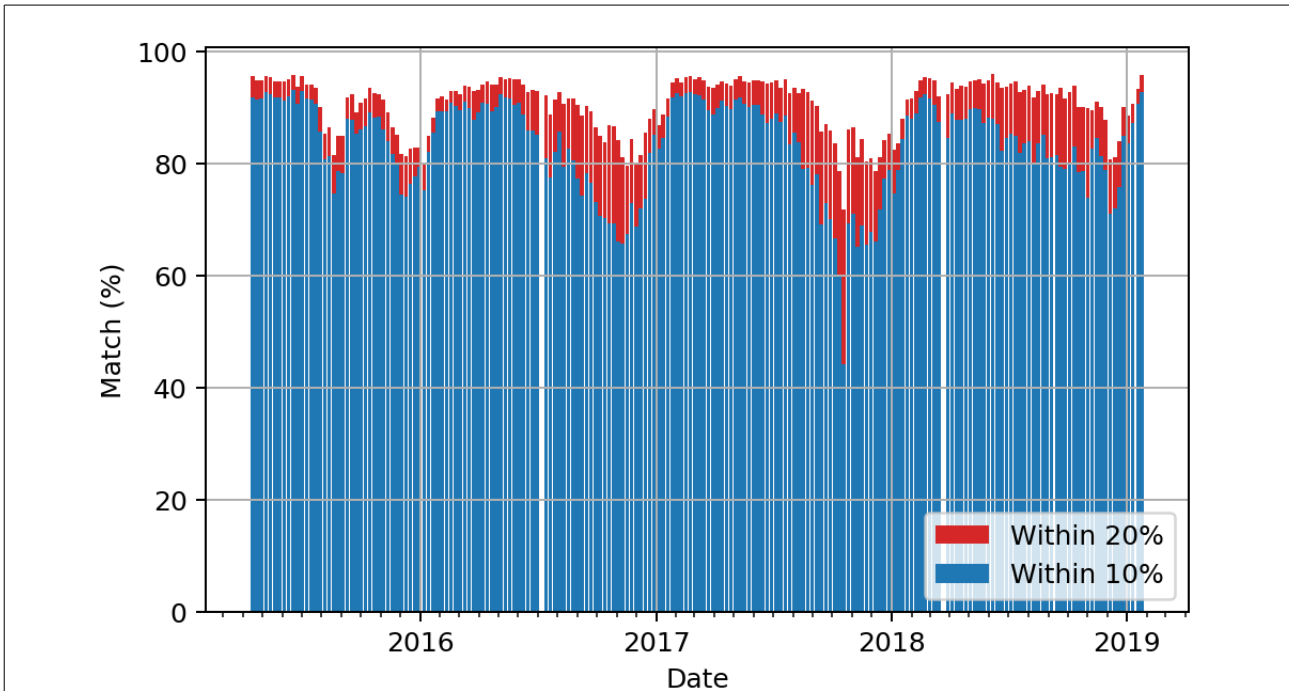


Figure 36: Southern Hemisphere match between OSI-430 and NIC ice charts; where OSI-430 ice concentration is within $\pm 10\%$ and $\pm 20\%$ of the NIC ice concentration.

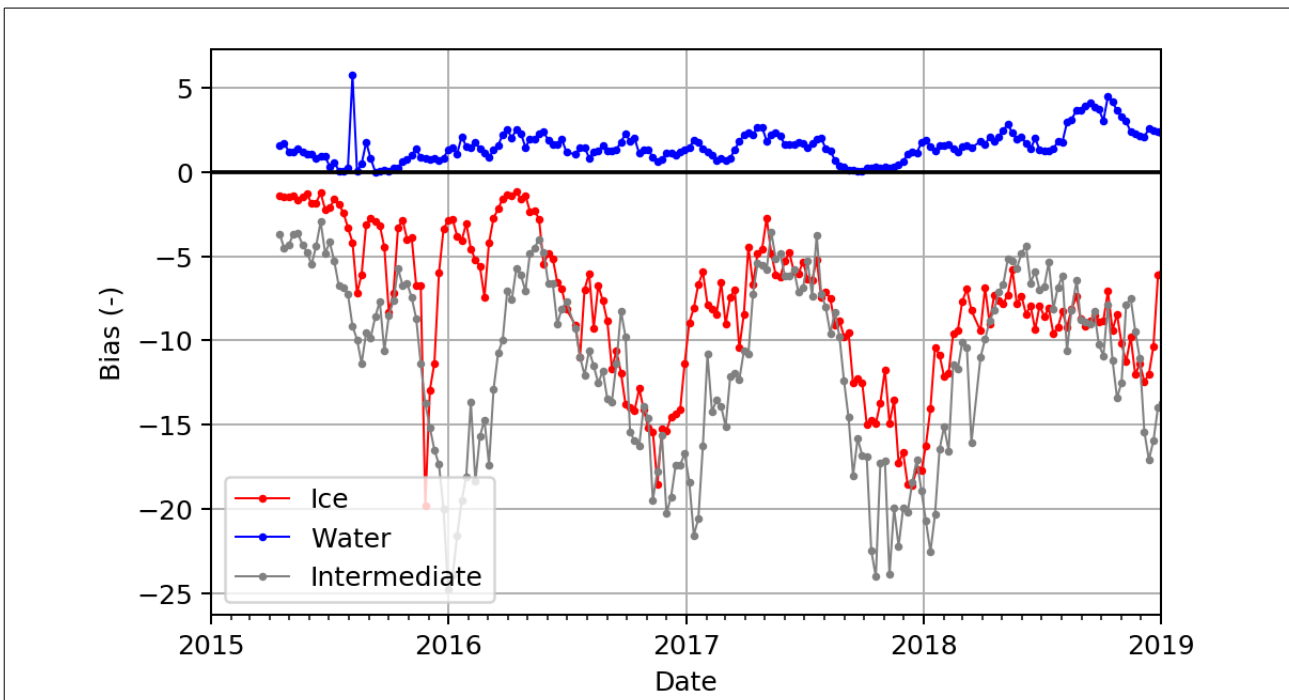


Figure 37: Southern Hemisphere difference (bias) between OSI-430 and NIC ice charts: where NIC shows ice ($>99\%$ ice), intermediate ($99\% < \text{ice} > 0\%$) and water (0% ice).

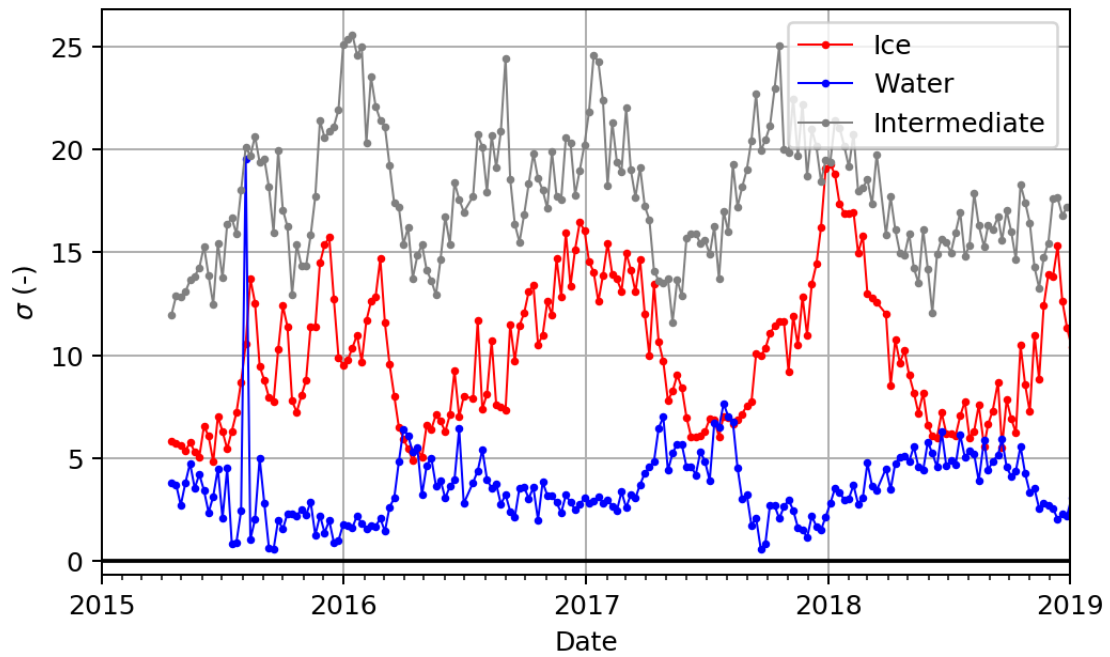


Figure 38: Southern Hemisphere standard deviation between OSI-430 and NIC ice charts: where NIC shows ice (>99% ice), intermediate (99%< ice >0%) and water (0% ice).

3. Comparison of sea ice area and extent monthly trends

In this chapter we compare three sources of hemispheric Sea Ice Extent (SIE) and Area (SIA) monthly variations and trends for the period 1979-2015. The three sources are the new CDR OSI-450, the previous CDR version (OSI-409 series) and the SIC CDR v2 from NSIDC [RD-5]. Since neither SIA nor SIE have ground-truth estimates, this section is not intended as a validation of OSI-450. It documents rather a comparison to two other sources of the climate trends observed by the new CDR.

3.1. SIC CDR data sources

3.1.1. OSISAF CDR v2 : OSI-450 and OSI-430-b

This is the new CDR dataset delivered by OSI SAF. OSI-450 differs from the previous CDR (OSI-409) on several areas: the sea ice concentration algorithm has been changed, the resolution is different (25 km vs 12 km), and the coastal interpolation has been improved. There is also an open water filter applied in OSI-450, though this should have little effect on calculations of SIA/SIE since they only count grid cells with at least 15% concentration while the filter is tuned to filter at an average 10% concentration. The CDR v2 covers 1979 to 2015.

3.1.2. OSISAF CDR v1 : OSI-409 and OSI-430 series

The previous CDR, OSI-409, covers the period 1979 - April 2015. For the purpose of comparing SIE and SIA through 2015, data from OSI-430 is used from April 20 2015 to complete the OSI-409 series for 2015. OSI-430 is the Interim Climate Data Record extending OSI-409 with a 31 days delay. It uses the exact same processing chain and algorithms as the CDR OSI-409, but applied on near-real-time satellite and NWP data streams. In the following we will use "OSI-409" to describe the combination of these two data sources.

3.1.3. NSIDC SIC CDR V2 :

The NSIDC dataset *NOAA/NSIDC Climate Data Record of Passive Microwave Sea Ice Concentration* covers 1978 to 2015 at 25 km resolution. The files contain 4 different sea ice concentration variables. The SIC variable used for comparison in this report is the daily Merged NT/BT sea ice concentrations (goddard_merged_seaice_conc). The merged record has undergone some manual quality control and does therefore not meet the strict definition of a CDR. More information can be found at http://nsidc.org/data/docs/noaa/g02202_ice_conc_cdr/index.html

3.2. Definitions and Methodology

3.2.1. Indicators and trends

Sea Ice Extent (SIE) is defined as the area covered by sea ice, that is the area of ocean having at least 15% Sea Ice Concentration (SIC). Sea Ice Concentration is the fractional coverage of a grid cell that is covered with sea ice. Sea Ice Area (SIA) is the sum of the area of each grid cell multiplied by the fractional concentration for that cell.

The monthly SIE and SIA values discussed in this report is computed from daily SIE or SIA values, respectively. All sea ice covered ocean is included, lake ice is not.

Relative trends are computed with respect to the mean value during a reference period 1981-2000, which is the same as that used for the NSIDC Sea Ice Index. All the trends are from least-square linear regression, with no consideration for statistical correlations between the points along the time series. As for all trends, they describe the past changes, but should be used with caution when predicting future evolution. The linear rate of change is indicated as thousands km² per year, The rate of change is also reported as percentage change per decade, relative to the reference period.

3.2.2. Gap-filling and interpolation of missing daily SIC values

Both OSI SAF data records (OSI-409 and OSI-450) use spatio-temporal interpolation to fill potential data gaps in the daily maps of SIC. Such interpolation is used both in areas where there never is any satellite observations (the polar observation hole in the Northern Hemisphere), and where missing satellite data leave some regions and patches empty in the daily maps. This is especially the case for lower latitude coverage in the SMMR period (1978-1987) due to the narrower swath of the instrument. All these interpolated data are used for computing the SIE/SIA values reported in this section. On that topic, it is noteworthy that the OSI SAF data records both use all DMSP platforms (for SSM/I and SSMIS instruments) available at any time, which greatly reduces the occurrence of occasional missing SIC data.

On the contrary, the NSIDC SIC CDR processes only one DMSP platform at any time, and thus does not take advantage of the overlap of satellite missions. In addition, the NSIDC SIC CDR does not implement interpolation of missing data, neither at the polar observation hole, nor at occasional gap locations. Before computing the SIE/SIA values from this CDR, we filled the polar observation hole with 100% sea ice concentration. The other data holes due to missing satellite data are not interpolated for this CDR.

Some consequences on the SIE/SIA values are:

- The OSI SAF values can be larger than those from NSIDC because of the use of the overlapping missions and the interpolation of missing values;
- The contribution in SIA values from the polar observation holes might be slightly less for the OSI SAF than for the NSIDC CDR;
- Since the extent of the polar observation hole changes drastically from SMMR to SSM/I (and less from SSM/I to SSMIS), jumps in SIA might be observed for NSIDC (especially in 1987) and to a lesser extent for the OSI SAF values.

This should be kept in mind when viewing and discussing the SIE/SIA curves and trends presented in the remaining of this section.

3.2.3. Grids, Projections, land-masks, and climatologies

It is noteworthy that the three sources of SIC all have different grid extend, projection, grid spacing, land-mask, and applied maximum extent climatologies. Each of these differences might have effects on the computed SIE/SIA values. In this study we did not attempt to correct for any of these differences, and the daily SIE/SIA values are computed on the original product grid, and -thus- based on different land-masks and climatologies.

Differences in land-mask have a large impact on the difference in absolute SIE/SIA values since the number of ocean grid cells to be summed up is different. In the Northern Hemisphere, the number of coastal cells varies with season inside the maximum extent climatology, The differences in SIE/SIA values due to differences in land-masks will thus vary with month/season. This is much less pronounced in the Southern Hemisphere because all coast are “within” the sea ice. We note that the OSI-450 mask was designed to be more compatible to that of the NSIDC SIC CDR, and that this was not in focus for OSI-409.

All these differences, and especially that with land-masks make it difficult to compare absolute SIE/SIA values between the sources, which is why the results and analysis below focus on their trends.

3.3. Results

The main focus here is on comparing the Arctic and Antarctic SIE and SIA trends and relative differences for the 3 sources. Plots of the monthly SIE/SIA (based on the mean of the daily values) are shown for March and September. The curves representing OSI-450 are labelled “OSICDR2e”, curves representing OSI-409 are labelled “OSICDR1-12km”, and curves representing the CDR from NSIDC are marked “NSIDC-GD-MGD”. In addition, monthly trend values are presented in 1 and 2 found in Appendix A.

3.3.1. Northern Hemisphere SIE

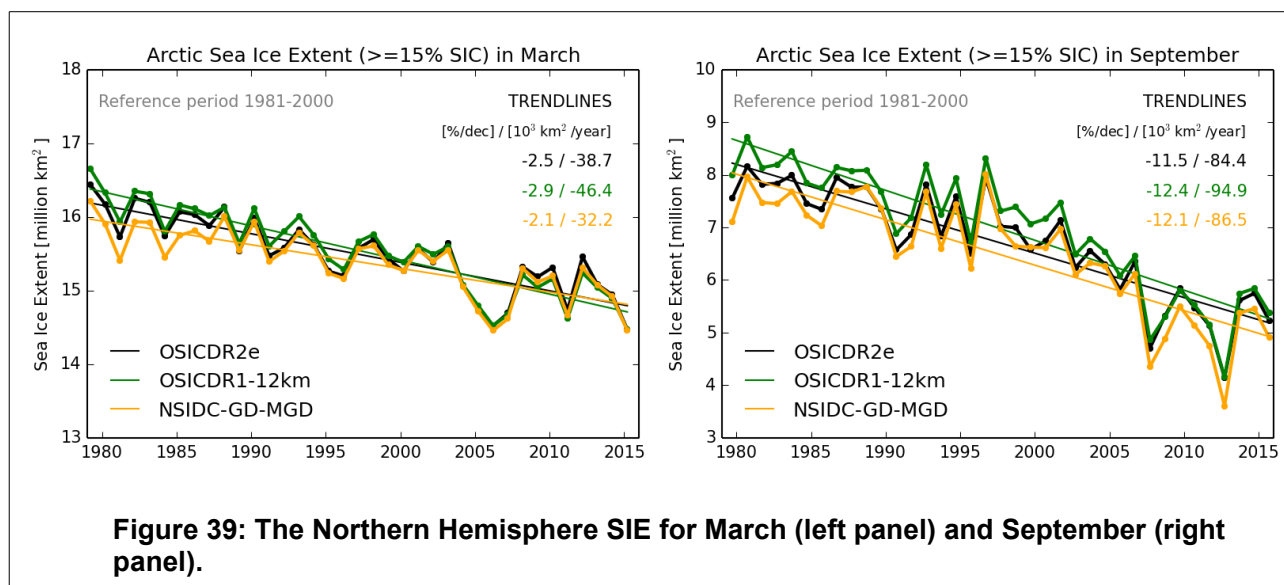
The Arctic monthly SIE from NSIDC is generally lower than the SIE from the two OSI SAF datasets for almost the entire period of comparison. The OSI-450 monthly SIE values and monthly trends are generally closer to NSIDC than what is the case for the OSI-409 values. For all months, OSI-409 shows the strongest, negative trend in SIE. NSIDC shows the weakest trends, except for July to September, when the OSI-450 monthly SIE trend is slightly weaker.

a) Northern Hemisphere SIE March

The Northern Hemisphere SIE for March is shown in the left panel of Figure 40. The two OSI SAF datasets produce very similar monthly SIE for March for the entire period of comparison. NSIDC produces slightly smaller March SIE values for the SMMR period (due to non-interpolated data gaps, see 40), after which monthly SIE from this dataset also follows the two other closely. March is the month of maximum ice extent. OSI-409 has the strongest, negative trend at -46.4 thousand km²/year, OSI-450 has a reduction of -38.7 thousand km²/year, and the NSIDC dataset gives a trend of -32.2 thousand km²/year.

b) Northern Hemisphere SIE September

The Northern Hemisphere SIE for September can be seen in the right panel of Figure 40. The new CDR (OSI-450) follows the variations in both OSI-409 and NSIDC closely for most of the period 1979-2015. During the SMMR period, OSI-450 shows September SIE values smaller than those from OSI-409 and larger than those from NSIDC. Entering the SSM/I period, OSI-450 follows NSIDC even closer up until 2006. From then on, OSI-450 and OSI-409 show almost identical monthly SIE values for September. OSI-450 and NSIDC have very similar trends, -84.4 thousand km²/year and -86.5 thousand km²/year, respectively. OSI-409 shows a stronger trend of -94.9 thousand km²/year.



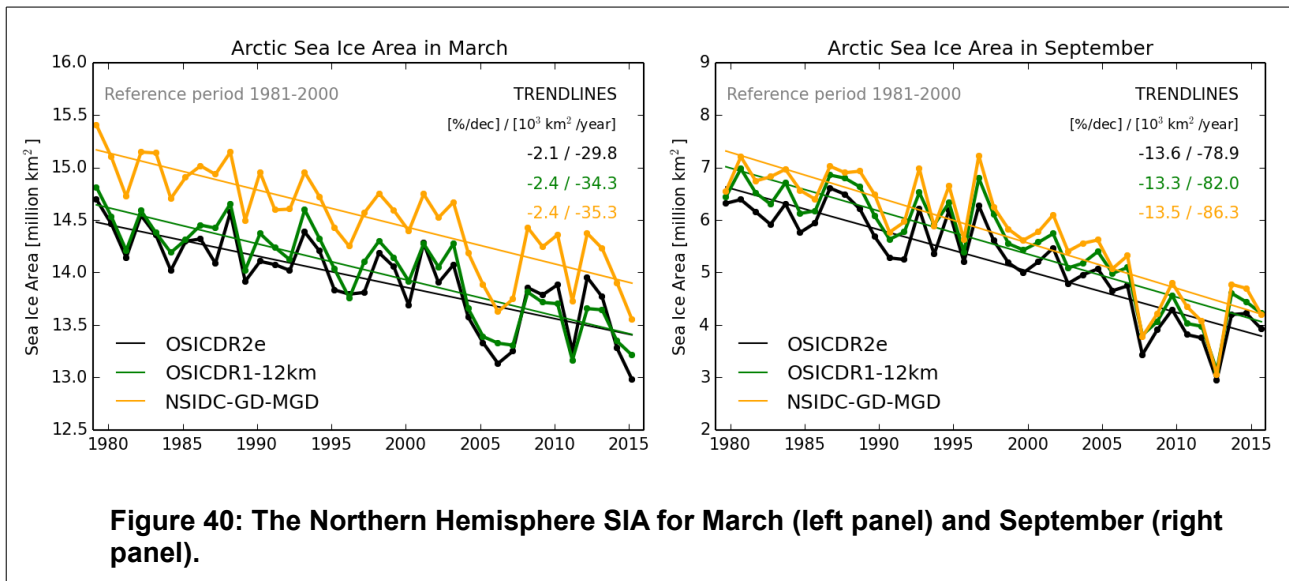
3.3.2. Northern Hemisphere SIA

When it comes to monthly Arctic SIA, NSIDC generally produces the highest SIA values. This is contrary to the situation for Arctic SIE where NSIDC gave the lowest SIE values for almost all months. This must mean that the NSIDC SIC CDR has larger values than the two OSISAF time-series for most months in the NH. OSI-450 has a tendency of giving rise to the smallest Arctic SIA values, with some exceptions where OSI-409 is slightly lower. OSI-409 is close / closer to OSI-450 for much of the year, but approaches NSIDC during the minimum ice period (August-October).

NSIDC has a stronger negative trend in SIA than OSI-450 for all months. Overall there is good agreement between the curves from all three sources.

a) Northern Hemisphere SIA March

For March, the month of maximum sea ice area, OSI-409 and OSI-450 are quite similar. NSIDC consequently produces the highest monthly March SIA, roughly 0.5 million km^2 above the SIA values from the OSI SAF datasets for the entire period of comparison. The three datasets give rise to similar trends for March SIA. NSIDC has the strongest negative trend at -35.3 thousand km^2/year , followed closely by OSI-409 at -34.3 thousand km^2/year . OSI-450 has a reduction in March SIA of -29.8 thousand km^2/year . The left panel of Figure 41 shows the Northern Hemisphere SIA for March.



b) Northern Hemisphere SIA September

The right panel of Figure 41 shows the Northern Hemisphere SIA for September. NSIDC produces the highest monthly September SIA (as was the case for March SIA), while OSI-450 produces the lowest monthly September SIA. The difference between OSI-450 and NSIDC remains relatively constant for the entire period of comparison, except for in 2012 where all three datasets produce an Arctic SIA minimum of approximately 3 million km². The trends range from -78.9 thousand km²/year (OSI-450), via -82.0 thousand km²/year (OSI-409) to -86.3 thousand km²/year (NSIDC).

3.3.3. Southern Hemisphere SIE

All three datasets show positive trends for Antarctic monthly SIE, and follow each other relatively well. In general, OSI-450 yields higher monthly SIE values than NSIDC. During Antarctic summer OSI-450 and OSI-409 produce very similar SIE.

a) Southern Hemisphere SIE March

The OSI SAF datasets show practically identical Antarctic SIE values for March, conf. the left panel of Figure 40. NSIDC shows the same temporal variation, but lies slightly lower in terms of absolute value. The trends in SIE are very similar. NSIDC has the strongest trend at 24.7 thousand km²/year, OSI-450 almost identical at 23.3 thousand km²/year, and the OSI-409 data yields a trend in SIE of 20 thousand km²/year.

b) Southern Hemisphere SIE September

OSI-450 has the highest monthly SIE values for September. The curves from all three datasets follow each other closely (conf. the right panel of Figure 40), except for some incidents where OSI-409 gives a suspiciously low SIE, due to some missing data that was not properly interpolated. As was the case for the March Antarctic SIE trends, the September trends are also very much the same at 24.1 thousand km²/year, 23.9 thousand km²/year and 23.7 thousand km²/year for OSI-450, NSIDC and OSI-409, respectively.

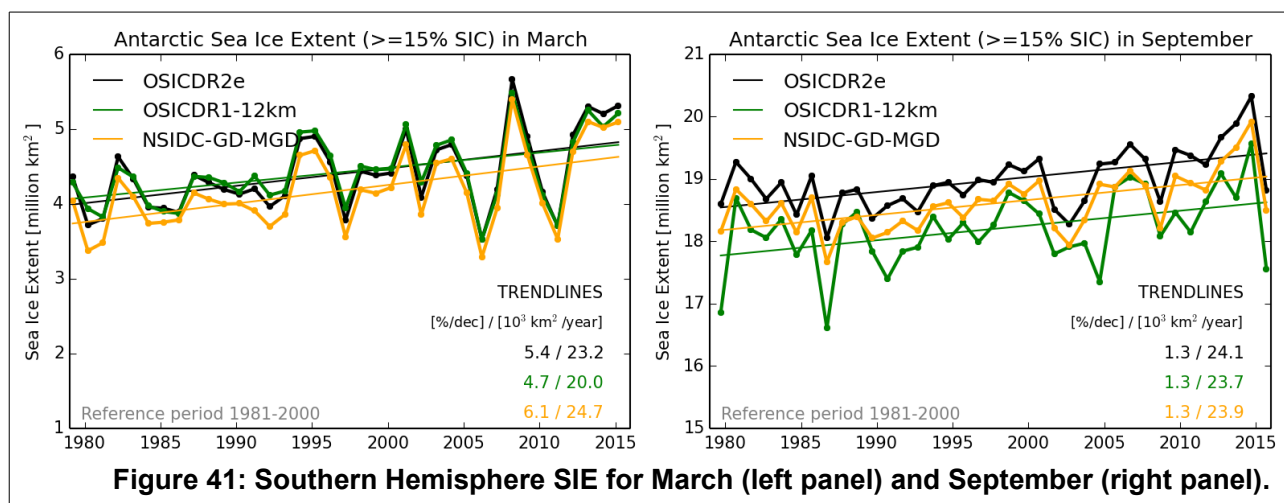


Figure 41: Southern Hemisphere SIE for March (left panel) and September (right panel).

3.3.4. Southern Hemisphere SIA

The SIA values are very similar for all three datasets during Antarctic summer (December - May), but the discrepancies are larger during the time of maximum Antarctic sea ice. During Antarctic winter, NSIDC generally produces the highest SIA values, followed by OSI-450.

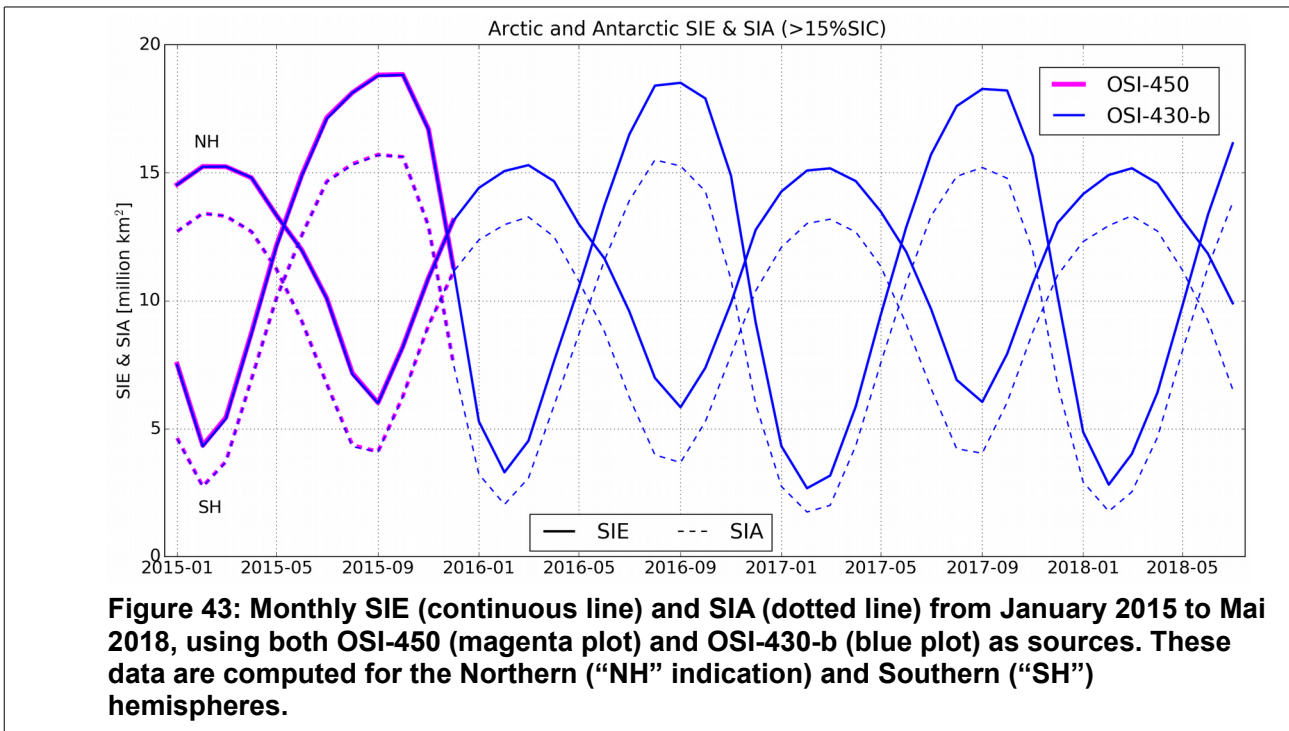
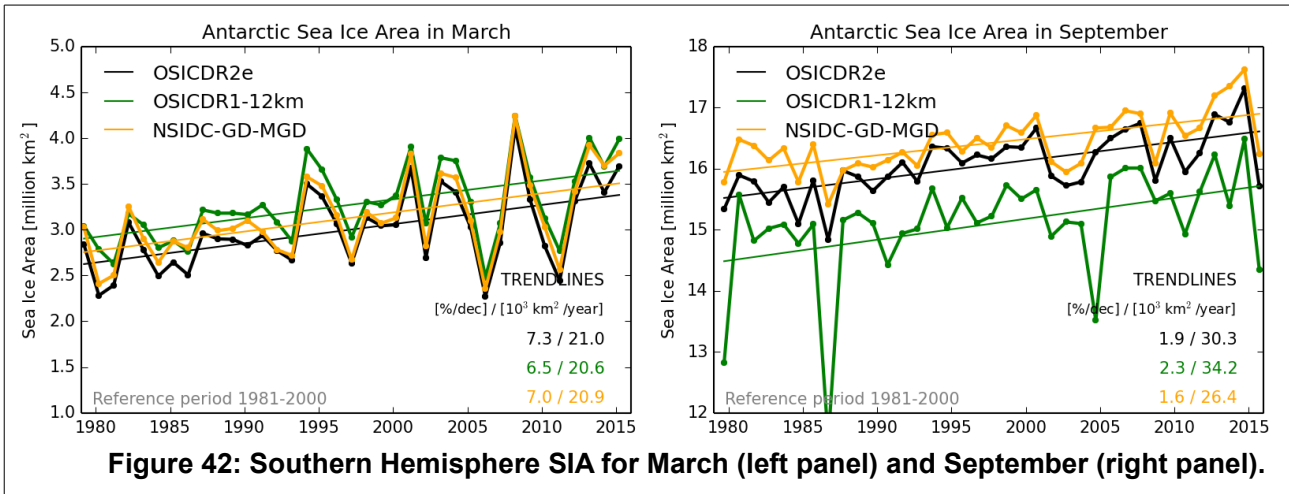
During Antarctic summer (Jan-March), OSI-409 produces larger Antarctic SIA values than the new OSI SAF CDR. From June to November, however, OSI-450 overtakes OSI-409. Generally, OSI-450 agrees more closely with NSIDC than what is the case for OSI-409.

a) Southern Hemisphere SIA March

All three datasets give more or less the same trend and yearly variation in Antarctic SIA for March. OSI-450 has a trend of 21 thousand km²/year, OSI-409 has a trend of 20.6 thousand km²/year, and the trend for NSIDC is 20.9 thousand km²/year. The left panel of Figure 44 shows the Southern Hemisphere SIA for March.

b) Southern Hemisphere SIA September

At maximum Antarctic ice extent, NSIDC shows the highest SIA values, approximately 1 million km² larger than OSI-409. OSI-450 is closer to NSIDC than to OSI-409. OSI-409 seems to suffer somewhat from missing data for September 1979, 1986 and 2004, and has the highest trend, 34.2 thousand km²/year. OSI-450 has a September SIA trend of 30.3 thousand km²/year, while NSIDC has a trend of 26.4 thousand km²/year. The Southern Hemisphere SIA for September is shown in the right panel of Figure 44. Comparison to the equivalent SIE trends (Figure 44) reveals that OSI-409 generally has much lower SIC values than both NSIDC CDR and OSI-450, which is confirmed by visual inspection of several daily maps (not shown): for OSI-409, it was rare to observe 100% SIC locations in SH September.



3.4. Continuity of SIE and SIA time-series with OSI-430-b

Figure 43 shows the monthly values of SIE and SIA in both hemispheres, for all the months from January 2015 to July 2018, using the sources OSI-450 and OSI-430-b. The SIA and SIE values are almost identical for the period both OSI-450 and OSI-430-b data are available during the year 2015 –. The continuity of the series from 2015 to 2018 is excellent.

3.5. Discussion

This section presented an inter-comparison of hemispheric monthly SIE/SIA values and their trends for three different CDRs (OSI-450, OSI-409, and NSIDC CDR) over the period 1979-2015. Since there are no available ground-truth SIE/SIA observations, this section is not intended as a validation, but rather as a sanity check of the new SIC CDR once aggregated into large-scale climate indicators. In addition, there are many differences between the three sources in terms of grid, projection, land-masks, climatologies, and interpolation of data gaps which challenge the direct comparison of both absolute values (e.g. land-masks) and trends (e.g. more missing values in the SMMR era).

With these limitation in minds, some observations can be made.

The new CDR OSI-450 seems to show the same climate signal as the two CDR it is compared with here.

For Arctic SIE, the new CDR is closer to the NSIDC CDR than the previous OSI SAF CDR was. This is not a goal per se, but seems to indicate that the strategies adopted in OSI-450 to prepare a land-mask and maximum ice climatology that are compatible with those of the NSIDC CDR was successful. For Antarctic SIE, the two OSI SAF CDRs take turn in being closer to the SIE from NSIDC. The new CDR has improved the agreement with NSIDC from August to November (see Appendix A). For the remaining months, all three show similar temporal variation in monthly Antarctic SIE.

When it comes to Arctic SIA all three datasets show very similar temporal variation for the entire period of comparison. NSIDC consequently gives the highest Arctic SIA values, which is not a surprise considering that its SIC values are computed as the maximum of two other algorithms (namely Bootstrap and NasaTeam). The NSIDC very often saturates at 100% SIC. In the Antarctic, the datasets also compare well, and the agreement in trend values are particularly good at ice minimum.

The ICDR continuity for the SIE and SIA series from 2015 to 2018 is well ensured using the OSI-450 and OSI-430-b sources.

4. Monitoring stability and internal consistency

In this section, we introduce and comment on a selection of time-series plots to document the temporal stability of the SIC CDR OSI-450, and the consistency with OSI-430-b. The text for OSI-450 is largely inspired by section 4.2.1 in Lavergne et al. (2019).

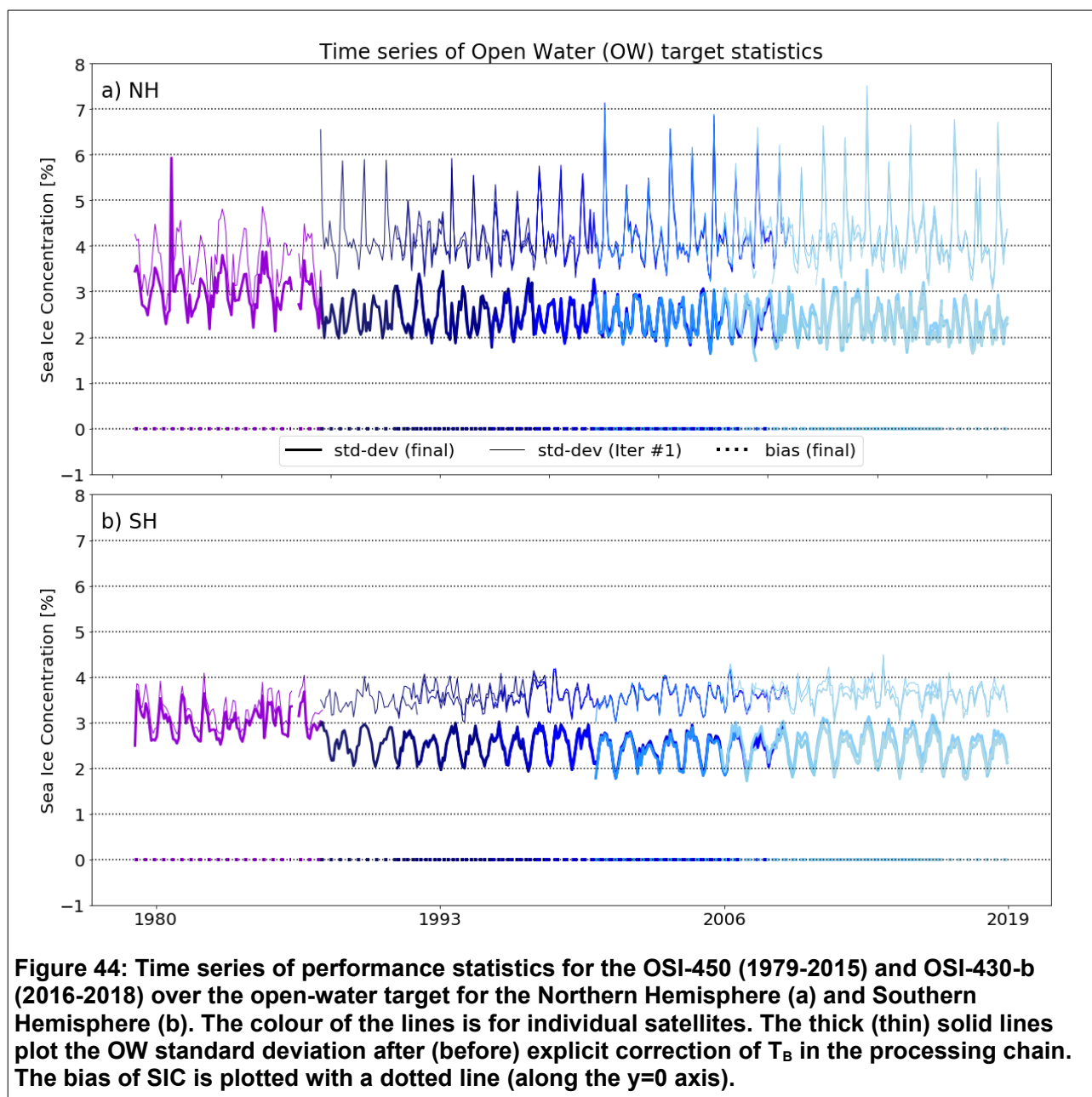
4.1. Long-term stability

Many time-series plots can be produced to illustrate the stability and internal consistency of the three CDRs. As an example, Fig. 44 shows the time series of the algorithm training statistics at the open-water target. As described in the ATBD, the algorithms implemented in the SIC CDRs dynamically tune their parameters to yield zero bias and minimum standard deviation of the computed SICs (a.k.a. best accuracy) over the open-water (OW) and closed-ice (CI) training targets. Figure 44 shows the Northern Hemisphere (NH, top) and Southern Hemisphere (SH, bottom) temporal evolution of the standard deviation (solid lines) and bias (dotted lines) of the SIC algorithms over OW target areas. The colour of the lines represents the satellite mission (from SMMR: purple, to SSMIS F18: light blue). Both OSI-450 (1979-2015) and OSI-430-b (2016-2018) are plotted. Prior to further describing Fig. 44, it is important to note that the biases and standard deviations discussed here are internal to the processing chains, not an evaluation of the CDR against independent observations of SICs (as is otherwise covered in this report).

From Fig. 44, it is easy to see that the algorithms implemented in the OSI-450 and OSI430-b CDRs achieve zero bias (dotted lines along the $y=0$ axis) for all instruments and for both hemispheres. Achieving zero bias despite the changes in central wavelengths and calibrations from one satellite to the next is one of the key advantages of using dynamically tuned algorithms (ATBD).

The impact of the explicit correction of brightness temperature for atmospheric noise effects is also clearly visible in Fig. 44, since the standard deviations resulting from uncorrected T_B data (thin solid lines) are consistently above those for corrected T_B data (thick solid lines) by about 3 % to 4 % on average, depending on the season and hemisphere. The seasonal variability is also larger from the uncorrected data, especially in the NH. It is noteworthy that the atmospheric noise reduction step does not much improve the OW standard deviation in the SH at the beginning of the OSI-450 period for the SMMR instrument (1979–1987). This is discussed in more details in Lavergne et al. (2019, section 4.2.1).

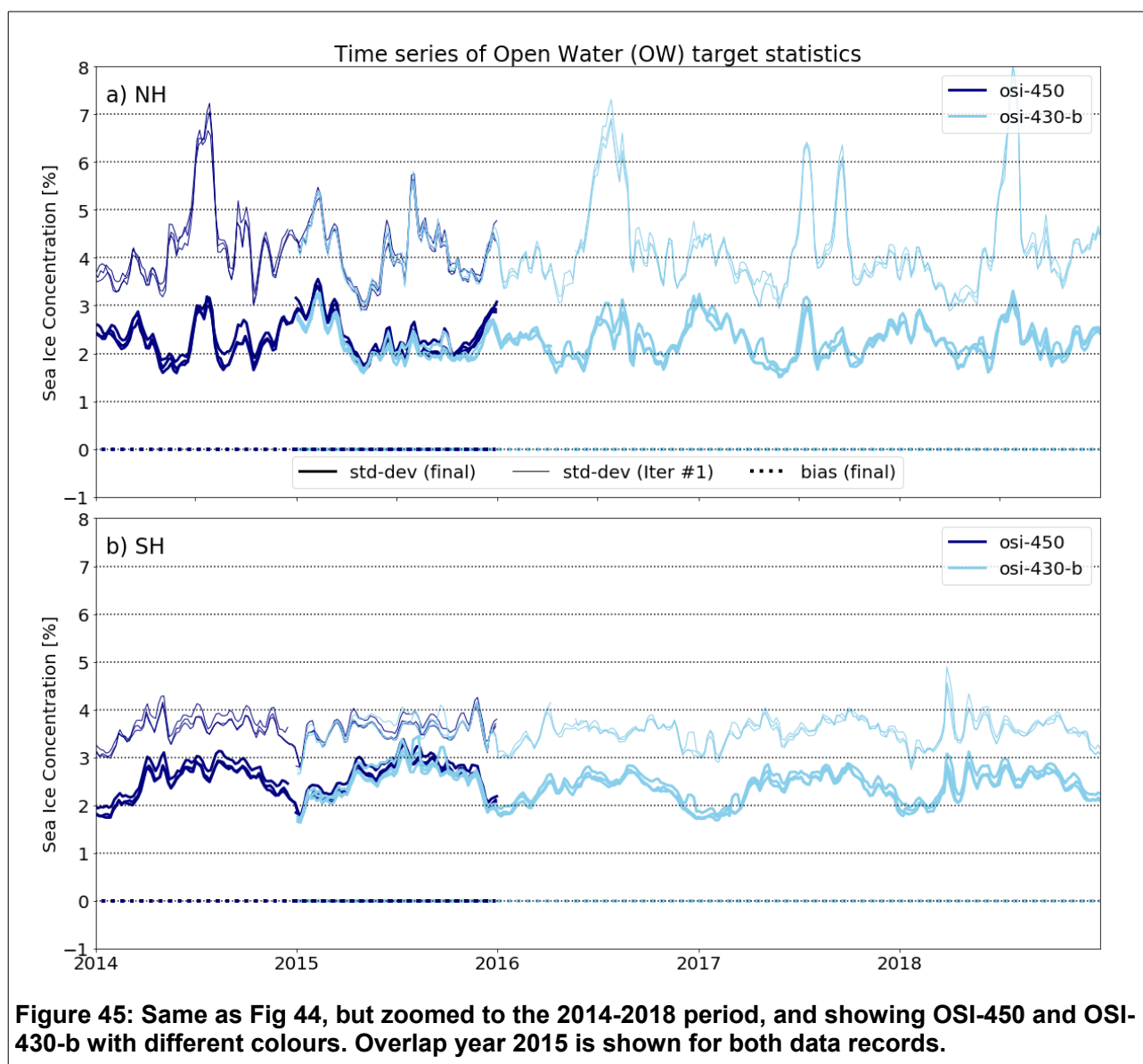
The time series in Fig. 44 illustrate that the algorithms behave as expected across satellite missions and are effectively tuned to achieve zero bias and a small retrieval noise for each instrument in the time series. Fig. X does not reveal jumps between OSI-450 and OSI-430-b, this this documented in more details in the next section.



4.2. Transition from OSI-450 to OSI-430-b, and stability of OSI-430-b

Figure 44 looks in more details at the transition between OSI-450 and OSI-430-b, and the stability during the first 3 years of OSI-430-b. It is important to look at the stability for at least two reasons: a) the input satellite data source for OSI-430-b is an operational data stream lacking most of the quality checks running in the Fundamental Climate Data Record (FCDR) used for OSI-450 (Fennig et al., 2017); b) the ECMWF analysis forecast system is updated regularly and this could introduce jumps.

Looking at the overlap year 2015, the transition is remarkable, both before and after atmospheric correction, despite both the satellite and weather data stream differ between OSI-450 and OSI-430-b. The further evolution over the period 2016-2018 does not reveal sharp transitions. Of particular interest, no such transitions are observed around the dates where the ECMWF operational system was upgraded (on 8/3/16, 22/11/16, 11/7/17 and 5/6/18 - see ECMWF [website](#) for relevant impacts on 2m temperature, surface winds, and atmospheric humidity). The impact of weather correction is on the distance between the un-corrected and corrected data (thin and solid), and this does not vary in the 4 years (except for seasonal variations). Such plots further strengthen our confidence in the atmospheric correction scheme, coupled with the dynamic tuning of the algorithms.



5. Conclusions

There are two scientific requirements listed in the Product requirement document table OSI-PRD-PRO-200: (i) the requirement on spatial resolution and (ii) the accuracy of the product on a yearly basis. Here the accuracy of the OSI SAF ice concentration products are evaluated using ice chart information for comparison.

- (i) The requirement on spatial sampling applying to the OSI SAF reprocessed ice concentration products are 25km. This requirement is met for both the OSI-450 and the OSI-430-b.
- (ii) The requirement on target accuracy, that applies to the OSI SAF reprocessed ice concentration products are a standard deviation yearly average of 8% for both the NH product and SH product.

OSI-450:

For the Northern Hemisphere, comparisons with ice charts give standard deviations of 5% for ice and 8% for water. The OSI-450 product thus meets the requirement on target accuracy for ice and water categories. With a total standard deviation yearly average of 5% for ice, this category is even within the optimal accuracy.

For the Southern Hemisphere the standard deviation is 7% for water and hence the target accuracy is met. With a total standard deviation yearly average of 10% for ice, this category is a bit above the target accuracy, but within the threshold accuracy. Table below summarizes comparison results:

	Match [%]		Bias [%]			Stddev [%]		
	within 10pct	within 20pct	ice	water	intermediate	ice	water	intermediate
Yearly average								
OSI-450 NH	82	90	-2	2	-7	5	8	17
OSI-409 NH	79	88	-3	7	-6	5	8	16
OSI-450 SH	85	90	-5	1	-10	10	7	18
OSI-409 SH	80	88	-6	3	-10	10	8	18

The new OSI-450 product performs better than the OSI-409 product in the comparison with ice charts for both hemispheres and both over ice and water. Standard deviations with regards to IAC are within the same range for both OSI SAF products, but OSI-450 performs better in the analysis of bias for the ice and water categories, as well as in percentage match within $\pm 10\%$ and $\pm 20\%$ of the IAC.

It is clear that the ice charts do not necessarily represent the truth, rather a fairly independent dataset for comparison. From October 2013 and on there is a better correspondence between the two data sets. This is likely due to the increase in frequency in NIC ice chart production for both hemispheres.

So, since the OSI-450 meets the requirements except for ice in Southern Hemisphere where it is a bit above, and it is better than OSI-409, the OSI-450 is ready to be released.

Comparisons of trends in sea ice extent and sea ice area show that the OSI-450 yields the same climate signal as OSI-409 and the CDR from NSIDC. The time series all show similar year-to-year variations, although there are systematic differences/biases between the products which are seasonally dependant.

OSI-430-b:

For the Northern Hemisphere, comparisons with ice charts in the years 2015-2017 give standard deviations of 7% for ice and 9% for water. The OSI-430-b product thus meets the requirement on target accuracy for the ice category. The result for the water category is a bit above the target accuracy, but within the threshold accuracy.

For the Southern Hemisphere the standard deviation is 3% for water and hence the target accuracy is met (this category is even within the optimal accuracy). With a total standard deviation yearly average of 11% for ice, this category is a bit above the target accuracy, but within the threshold accuracy. Table below summarizes comparison results:

2015 - 2017	Match [%]		Bias [%]			Stddev [%]		
	within 10pct	within 20pct	ice	water	Intermediate ice	ice	water	Intermediate ice
yearly average								
OSI-430-b NH	87	91	-3	2	-6	7	9	14
OSI-430-b SH	85	91	-8	0	-11	<u>11</u>	3	17

The tables below summarize the validation statistics of OSI-430-b compared to those of the OSI-450 in 2015 and the OSI-430 in 2016-2017, respectively. It is shown that the OSI-430-b performs equally good as the OSI-450 when comparing the yearly average validation statistics and for both hemispheres (for all statistical parameters the differences are on the first decimal).

2015	Match [%]		Bias [%]			Stddev [%]		
	within 10pct	within 20pct	ice	water	Intermediate ice	ice	water	Intermediate ice
yearly average								
OSI-430-b NH	88	92	-2	2	-5	6	7	13
OSI-450 NH	88	92	-2	2	-5	6	7	13
OSI-430-b SH	88	92	-4	0	-9	<u>10</u>	3	15
OSI-450 SH	88	92	-4	0	-9	11	<u>3</u>	<u>14</u>

When comparing OSI-430-b to the OSI-430, it is clear from the validation statistics that the new ICDR performs better than its predecessor for the Northern Hemisphere. Especially the biases on the ice and water categories have decreased somewhat in OSI-430-b, compared to OSI-430.

For Southern hemisphere, the validation statistics show that the new ICDR overall performs better than its predecessor for the match categories. Also for the water category the new ICDR overall performs better than the old ICDR. For the ice category, the 2016-2017 yearly average biases are at the same level, but the standard deviation on the bias has increased with the OSI-430-b, compared to the OSI-430. Please bear in mind that these ICDR comparison results cover a relatively short period (2016-2017) and that interannual variability can have a strong effect on the results. In that context, there are not large differences in the performance of the OSI-430-b and the OSI-430, even for the Southern Hemisphere.

2016 -2017	Match [%]		Bias [%]			Stddev [%]		
	within 10pct	within 20pct	ice	water	Intermediate ice	ice	water	Intermediate ice
yearly average								
OSI-430-b NH	<u>86</u>	<u>91</u>	<u>-4</u>	<u>2</u>	-6	<u>7</u>	<u>9</u>	14
OSI-430 NH	81	88	-6	8	-6	8	12	14
OSI-430-b SH	<u>84</u>	<u>91</u>	-9	1	<u>-12</u>	12	4	<u>18</u>
OSI-430 SH	82	90	-9	1	-13	<u>10</u>	<u>3</u>	19

The SIE and SIA series computed using OSI-450 and OSI-430-b, show an excellent match between both sources.

We also show selected time-series plot of parameters internal to the SIC algorithm tuning and document that the stability of the algorithms is good both over the whole OSI-450 period, at the transition to OSI-430-b, and during the first 3 years of OSI-430-b despite changes in the ECMWF weather forecast system.

So, the OSI-430-b meets the requirements, except for requirement on water in the Northern Hemisphere and ice in the Southern Hemisphere, both categories where being little above the target. Nevertheless, OSI-430-b is found to be temporally consistent with the OSI-450 and also found to be overall better than its predecessor; the OSI-430, especially for the Northern Hemisphere. Thus, the OSI-430-b is ready to be released.

6. Appendix

Northern Hemisphere						
Month	SIA			SIE		
	OSI-450	OSI-409	NSIDC	OSI-450	OSI-409	NSIDC
January	-36.2	-41.4	-41.4	-45.4	-53.3	-37.0
February	-33.4	-40.0	-40.2	-43.4	-50.9	-35.6
March	-29.8	34.3	-35.3	-38.7	-46.4	-32.2
April	-28.7	-33.2	-32.7	-34.3	-42.2	-29.8
May	-31.1	-38.5	-34.0	-32.0	-40.4	-26.5
June	-41.8	-59.3	-52.0	-42.4	-56.6	-41.4
July	-56.6	-70.1	-71.7	-64.9	-82.5	-69.4
August	-65.4	-80.1	-77.6	-72.2	-89.8	-75.2
September	-78.9	-82.0	-86.3	-84.8	-94.9	-86.5
October	-71.6	-78.0	-73.0	-67.5	-80.7	-65.1
November	-43.4	-51.3	-44.8	-46.7	-57.1	-40.6
December	-37.6	-43.3	-39.9	-41.7	-49.0	-34.0

Table 1: Monthly trends in sea ice area (SIA) and extent (SIE) in 10^3 km^2 per year for the Northern Hemisphere during the period 1979-2015 for OSI-450, OSI-409 and NSIDC.

Southern Hemisphere						
Month	SIA			SIE		
	OSI-450	OSI-409	NSIDC	OSI-450	OSI-409	NSIDC
January	22.7	23.8	18.4	33.3	32.0	24.3
February	12.5	13.1	10.2	16.5	15.4	13.3
March	21.0	20.6	20.9	23.2	20.2	24.7
April	35.7	44.3	33.7	28.9	37.9	30.4
May	38.6	37.3	37.2	32.6	31.0	33.8
June	38.2	45.7	36.9	28.2	32.9	31.5
July	32.0	31.5	30.7	23.5	19.5	26.5
August	26.6	25.3	23.8	19.7	13.7	20.4
September	30.3	34.2	26.4	24.1	23.7	23.9
October	32.2	33.4	26.6	24.3	30.5	23.6
November	26.1	16.7	20.8	19.4	17.8	18.3
December	26.5	21.3	22.6	30.0	26.9	25.7

Table 2: Monthly trends in sea ice area (SIA) and extent (SIE) in 10^3 km^2 per year for the Southern Hemisphere during the period 1979-2015 for OSI-450, OSI-409 and NSIDC.